ISTANBUL TECHNICAL UNIVERSITY ★ GRADUATE SCHOOL

EFFECT OF SELF-STEEPENING ON OPTICAL SOLITONS IN NONLINEAR MEDIA

M.Sc. THESIS

Eril Güray ÇELİK

Department of Mathematical Engineering

Mathematical Engineering Programme

FEBRUARY 2022

ISTANBUL TECHNICAL UNIVERSITY ★ GRADUATE SCHOOL

EFFECT OF SELF-STEEPENING ON OPTICAL SOLITONS IN NONLINEAR MEDIA

M.Sc. THESIS

Eril Güray ÇELİK
(509181212)

Department of Mathematical Engineering

Mathematical Engineering Programme

Thesis Advisor: Prof. Dr. Nalan ANTAR

FEBRUARY 2022

İSTANBUL TEKNİK ÜNİVERSİTESİ ★ LİSANSÜSTÜ EĞİTİM ENSTİTÜSÜ

DOĞRUSAL OLMAYAN ORTAMLARDA ÖZ-DİKLEŞTİRMENİN OPTİK SOLİTONLAR ÜZERİNDEKİ ETKİSİ

YüKSEK LİSANS TEZİ

Eril Güray ÇELİK
(509181212)

Matematik Mühendisliği Anabilim Dalı

Matematik Mühendisliği Programı

Tez Danışmanı: Prof. Dr. Nalan ANTAR

ŞUBAT 2022

Eril Güray ÇELİK, a M.Sc. student of ITU Graduate School student ID 509181212, successfully defended the thesis entitled "EFFECT OF SELF-STEEPENING ON OPTICAL SOLITONS IN NONLINEAR MEDIA", which he/she prepared after fulfilling the requirements specified in the associated legislations, before the jury whose signatures are below.

Thesis Advisor :	**Prof. Dr. Nalan ANTAR** Istanbul Technical University	.....
Jury Members :	**Prof. Dr. İlkay BAKIRTAŞ AKAR** Istanbul Technical University	.....
	Assist. Prof. Dr. Mahmut BAĞCI Yeditepe University	.....

Date of Submission : 13 January 2022
Date of Defense : 17 February 2022

To my family,

FOREWORD

I started my master's degree at Istanbul Technical University in 2019 and gained invaluable experiences during my time here. When I first met with my dear advisor, Prof. Dr. Nalan Antar, I understood that we would do a good job. Prof. Dr. Nalan Antar has led me to do research in a very important, up-to-date and modern area, and has never spared her help and support during the time we worked together. In addition, our collaborative Prof. Dr. İlkay Bakırtaş Akar contributed greatly to the development of my academic skills by sharing her knowledge and experience with me in every subject I needed. I am grateful to Prof. Dr. Nalan Antar and Prof. Dr. İlkay Bakırtaş Akar, the lead architects of this thesis, for all their contributions. I would also like to thank my friend Melis Turgut, with whom we are in the same working group, for all her help.

While preparing this thesis, Assist. Prof. Dr. Mahmut Bağcı and Assist. Prof. Dr. İzzet Göksel generously shared their previous work with me. Their work has guided me and made my job much easier. I would like to thank Assist. Prof. Dr. Mahmut Bağcı and Assist. Prof. Dr. İzzet Göksel for all their contributions. I hope this thesis will be a useful resource that other researchers can benefit from.

My family has always supported me throughout my education life. Thank you to my family for all their support. I will always carry their love in my heart.

Thank you very much to all my relatives, friends, and everyone who helped me. All of you have contributed to this work.

February 2022 Eril Güray ÇELİK

TABLE OF CONTENTS

Page

ABBREVIATIONS

CQNLS	**:** Cubic-Quintic Nonlinear Schrödinger
Eq.	**:** Equation
KdV	**:** Korteweg-de Vries
NLS	**:** Nonlinear Schrödinger
PSR	**:** Pseudospectral Renormalization
$\mathscr{P}\mathscr{T}$	**:** Parity-Time
SR	**:** Spectral Renormalization
SSFM	**:** Split-step Fourier Method

LIST OF FIGURES

Page

EFFECT OF SELF-STEEPENING
ON OPTICAL SOLITONS IN NONLINEAR MEDIA

SUMMARY

Optical solitons are solitary waves that propagate without deteriorating their special structures as a result of the balance between the group velocity dispersion effect and the nonlinear effect caused by the change in refractive index due to the Kerr effect. Soliton generation and analysis in optics is a pretty popular and modern research topic, as they have a wide range of applications, such as optical communication technology, optical sensing, pulse compression in ultrafast optics and all-optical switching. Particularly, the propagation of optical solitons in fiber optic communication systems is an area of great interest to researchers.

Optical solitons can propagate through long distances in fiber transmission systems without being affected by chromatic and polarization mode dispersion. Since their natural structure is preserved, they can be used as natural optical bits of information in fiber optic systems.

In nonlinear optics, the propagation of the light pulse in optical fibers can be modeled by the cubic-quintic nonlinear Schrödinger (CQNLS) equation. In fiber optic systems, the width of the optical pulses is reduced to increase the bandwidth and communication speed. Whereas, if the width of the light pulses is very small, that is, the frequency is high, the CQNLS equation may be insufficient to model the physical system. Because, if the light pulse is short, often some higher-order effects need to be taken into account. It can be said that the third-order dispersion, self-steepening (or nonlinear dispersion) and the Raman effect are the most significant higher order effects. The CQNLS equation with Raman effect and self-steepening effect can be written as

$$iu_z + \frac{\beta}{2}u_{xx} + \gamma_1 |u|^2 u + \gamma_2 |u|^4 u + is\frac{\partial}{\partial x}\left(|u|^2 u\right) + u\tau\frac{\partial}{\partial x}\left(|u|^2\right) = 0, \qquad \textbf{(1)}$$

where u is the envelope proportional to the electric field, x is the transverse coordinate, z is the distance along the direction of propagation, γ_1 is the coefficient of the cubic (Kerr-type) nonlinear term, γ_2 is the coefficient of the quintic nonlinear term, u_{xx} corresponds to diffraction and β is the diffraction coefficient, s is the self-steepening coefficient and τ is the Raman coefficent.

Equation (1) can be considered together with a complex potential which has parity-time ($\mathscr{P}\mathscr{T}$) symmetry. $\mathscr{P}\mathscr{T}$- symmetric systems are in equilibrium and have completely real energy levels. In an optical waveguide, the real part of the $\mathscr{P}\mathscr{T}$- symmetric potential corresponds to the spatial distribution of the refractive index, and the imaginary part corresponds to the balanced gain-loss relationship.

In this thesis we worked with the following $\mathscr{P}\mathscr{T}-$ symmetric potential:

$$V_{\mathscr{P}\mathscr{T}}(x) = V_0 \cos^2(x) + iW_0 \sin(2x), \tag{2}$$

where V_0 and W_0 are the depths of the real and imaginary parts of the potential, respectively.

NLS equations with higher-order effects can not be solved analytically. Therefore, this equations should be handled with numerical methods. In this thesis, the existence and stability of soliton solutions of some kind of NLS equations that have higher-order effects and the $\mathscr{P}\mathscr{T}$- symmetric potential were investigated numerically. The pseudospectral renormalization method was used to obtain fundamental soliton solutions. In order to test the nonlinear stability of solitons, spatial evolution simulation of solitons was examined. For this, the split-step Fourier method, which has a very high performance in NLS-type equations, was used. In addition, while examining the dynamic properties of solitons, linear stability conditions were also taken into account. Linear stability analysis of solitons was performed by examining the whole linear stability spectrum of solitons with the help of the Fourier collocation method. The first 4 chapters of this thesis give information about NLS equations, optical solitons, higher-order effects, numerical methods, and stability analysis.

In Chapter 5, the existence and dynamic properties of solitons obtained from the NLS equation with the self-steepening term are analyzed. In addition, the relationship between $\mathscr{P}\mathscr{T}$- symmetric periodic potential (2) and the influences of the self-steepening effect is examined. It has been observed that the $\mathscr{P}\mathscr{T}$- symmetric periodic potential helps to obtain stable solitons by eliminating adverse effects.

In Chapter 6, the soliton solutions of the CQNLS equation with the self-steepening term were investigated in the self-focusing cubic, self-defocusing quintic medium. It has been determined that the destabilization effect of self-steepening can be arrested when the coefficient of the cubic nonlinear term is 1 and the coefficient of the quintic nonlinear term is -1.

Finally, the conclusions of this thesis are summarized in Chapter 7.

DOĞRUSAL OLMAYAN ORTAMLARDA ÖZ-DİKLEŞTİRMENİN OPTİK SOLİTONLAR ÜZERİNDEKİ ETKİSİ

ÖZET

Lineer olmayan dispersif dalgalar, uzun yıllardan beri birçok bilimsel araştırmaya konu olmaktadır. Çoklu ölçek metodu gibi, fiziksel olayları yöneten lineer olmayan dalga denklemlerini türetmek için kullanılan bazı asimptotik yöntemlerin geliştirilmesiyle birçok alana yayılmış ve altmış yılı aşkın bir süredir hızlı bir gelişim göstermeye devam etmektedir. Korteweg-de Vries (KdV) denklemi ve doğrusal olmayan Schrödinger (NLS) denklemi, çoklu ölçek yöntemiyle elde edilen önemli denklemlerden birkaçıdır. Bu evrensel denklemler, biyoloji, katı hal fiziği, Bose-Einstein yoğunlaşması ve doğrusal olmayan optik gibi bilimin tüm dallarında karşılaşılan solitonlar da dahil olmak üzere bazı özel çözümlere sahiptirler.

Solitonlar, yayılım gösterirken grup hız dağılımı etkisi ile doğrusal olmayan etki arasındaki denge sonucunda şekilleri korunan tekil dalgalardır.

Optikte soliton üretimi ve analizi; optik iletişim teknolojisi, optik algılama, ultra hızlı optikte darbe sıkıştırma ve optik anahtarlama gibi çok çeşitli uygulamaya sahip olduğu için oldukça popüler ve modern bir araştırma konusudur. Özellikle, fiber optik haberleşme sistemlerinde optik solitonların yayılımı günümüzdeki teknolojik ihtiyaçlardan dolayı araştırmacıların büyük ilgi gösterdiği bir alandır.

Optik solitonlar, fiber iletim sistemlerinde kromatik ve polarizasyon modu dağılımından etkilenmeden uzun mesafeler boyunca yayılabilirler. Doğal yapıları korunduğu için fiber optik sistemlerde doğal optik bilgi bitleri olarak kullanılmaktadırlar.

Doğrusal olmayan optikte, ışık darbesinin optik fiberlerde yayılması, aşağıdaki kübik-kuintik doğrusal olmayan Schrödinger (CQNLS) denklemi ile modellenebilir:

$$iu_z + \frac{\beta}{2}u_{xx} + \gamma_1 |u|^2 u + \gamma_2 |u|^4 u = 0. \qquad \textbf{(3)}$$

Burada u elektrik alan ile orantılı zarfı, z optik darbenin yayılma yönünü, γ_1 doğrusal olmayan kübik terimin katsayısını, γ_2 doğrusal olmayan kuintik terimin katsayısını, u_{xx} kırınımı ve β kırınım katsayısını temsil etmektedir. Kırınım, bir ışık demetinin havadan veya bir kristalden geçerken mesafe boyunca genişlemesi olarak düşünülebilir. Optikte kırınım denilen bu terimin su dalgalarındaki karşılığı dağılım yani dispersiyondur.

Yukarıdaki denklemde γ_1 ve γ_2'nin pozitif veya negatif olmasına göre farklı ortamlar tanımlanabilir. Pozitif işaret, doğrusal olmayan optik sürecin kendine odaklı olduğunu, negatif işaret ise doğrusal olmayan optik sürecin kendine odaklı olmadığını gösterir.

Bu tezde kendine odaklı kübik ($\gamma_1 = 1$, $\gamma_2 = 0$) ve kendine odaklı kübik-kendine odaklı olmayan kuintik ($\gamma_1 = 1$, $\gamma_2 = -1$) ortamlar üzerinde çalışılmıştır.

Fiber optik sistemlerde, bant genişliğinin ve iletişim hızının arttırılabilmesi için optik darbelerin genişliğinin azaltılması, yani frekansın arttırılması gerekir. Ancak ışık darbelerinin genişliği femtosaniyeler ile ifade edilecek kadar küçük olduğunda CQNLS denkleminde modellenmeyen bazı lineer ve lineer olmayan etkiler çok önemli bir hale gelir. Bunlardan en önemlilerinin üçüncü mertebeden dispersiyon, öz-dikleşme (lineer olmayan dispersiyon) ve Raman etkisi olduğu söylenebilir. Raman etkisi ve öz-dikleşme etkisi ile modellenen CQNLS denklemi aşağıdaki biçimde yazılabilir:

$$iu_z + \frac{\beta}{2}u_{xx} + \gamma_1 |u|^2 u + \gamma_2 |u|^4 u + is\frac{\partial}{\partial x}\left(|u|^2 u\right) + u\tau\frac{\partial}{\partial x}\left(|u|^2\right) = 0. \tag{4}$$

Bu denklemde, s öz-dikleşme terimi katsayısını, τ ise Raman terimi katsayısını temsil etmektedir. Hem s hem de τ darbe genişliği ile ters orantılıdır. Bu katsayılar ile darbe genişliği arasındaki ilişki aşağıdaki formülden açıkça görülmektedir.

$$s = \frac{1}{\omega_0 T_0}, \tau = \frac{T_R}{T_0}. \tag{5}$$

Burada, T_R Raman kazanç spektrumunun eğimi ile ilgili Raman katsayısı, T_0 darbe genişliği, $\omega_0 = \omega(k_0)$ ve k_0 dalga paketinin baskın dalga sayısı, $\omega = \omega(k)$ ise $e^{i(kx-\omega t)}$ Fourier dalgası için doğrusal dağılım ilişkisidir.

Denklem (4) parite-zaman ($\mathscr{P}\mathscr{T}$) simetrisine sahip bir kompleks potansiyel ile birlikte düşünülebilir. $\mathscr{P}\mathscr{T}$ simetrisine sahip sistemler ortamdan izole olmasa bile dengede olurlar. Yani etraftan kazandıkları enerji ile etrafa verdikleri enerji birbirine eşittir. Bir optik dalga kılavuzunda, $\mathscr{P}\mathscr{T}$- simetrik potansiyelin gerçek kısmı, kırılma indisinin uzaysal dağılımına, sanal kısımı ise dengeli kazanç-kayıp ilişkisine karşılık gelir. Bu tezde aşağıdaki $\mathscr{P}\mathscr{T}$- simetrik periyodik potansiyel kullanılmıştır:

$$V_{\mathscr{P}\mathscr{T}}(x) = V_0 \cos^2(x) + iW_0 \sin(2x), \tag{6}$$

V_0 ve W_0 sırasıyla potansiyelin gerçek ve sanal kısımlarının derinlikleridir.

Yüksek dereceden etkilere sahip NLS denklemleri analitik olarak çözülemez. Dolayısıyla bu denklemler ile çalışılırken nümerik yöntemler büyük önem arz etmektedir. Bu tezde öz-dikleşme etkisine ve $\mathscr{P}\mathscr{T}$- simetrik potansiyele sahip çeşitli NLS denklemlerinin soliton çözümleri ve kararlılık analizleri nümerik olarak incelenmektedir. Temel soliton çözümlerin bulunabilmesi için yarı-spektral yeniden normalleştirme (PSR) metodu kullanılmıştır. Elde edilen solitonların lineer olmayan kararlılık analizi, solitonlar z yönünde ilerletilip yapısında meydana gelen değişiklikler incelenerek yapılmıştır. Bu işlem için, NLS-tipi denklemlerde oldukça yüksek performans gösteren ayrık-adımlı Fourier yöntemi (SSFM) tercih edilmiştir. Ayrıca, bu çalışmada solitonların dinamik özellikleri incelenirken lineer kararlılık analizine de yer verilmektedir. Solitonların lineer kararlılık analizi, Fourier kollokasyon metodu yardımı ile solitonların lineer stabilite spektrumu incelenerek yapılmıştır.

Bölüm 1'de NLS denklemlerinin yapısından, kullanım alanlarından ve tarihsel gelişimlerinden bahsedilmektedir. Ayrıca tezde çalışılacak olan denklemler hakkında ön bilgiler verilmektedir.

Bölüm 2'de optik solitonların genel yapısı, kullanım alanları ve fiber optik iletişimdeki önemleri anlatılmaktadır. Ayrıca $\mathscr{PT}$ simetri kavramı, optik kafeslerde solitonlar ve optik solitonlar üzerinde meydana gelebilecek bazı yüksek dereceden etkiler tanıtılmaktadır.

Bölüm 3'te bu tezde kullanılan nümerik yöntemler yer almaktadır. İlk olarak; öz-dikleşme etkisine, Raman etkisine ve $\mathscr{PT}$- simetrik potansiyele sahip CQNLS denkleminin PSR yöntemi ile çözümü anlatılmıştır. Daha sonra ayrık-adımlı Fourier yönteminin ve Fourier kollokasyon yönteminin NLS denklemine uygulanışı gösterilmiştir.

Bölüm 4'te lineer olmayan stabilite ve lineer stabilite kavramları açıklanmaktadır. Ayrık-adımlı Fourier yönteminin; öz-dikleşme etkisine, Raman etkisine ve $\mathscr{PT}$-simetrik potansiyele sahip CQNLS denklemine uygulanışı anlatılmaktadır. Ayrıca solitonların lineer spekrumunu bulmak için kullanılacak bir özdeğer problemi geliştirilmiştir.

Bölüm 5'te öz-dikleşme terimine sahip NLS denkleminin, s katsayısının değerlerine göre soliton çözüme sahip olduğu aralıklar bulunmuştur. Daha sonra öz-dikleşme etkisinin solitonların stabilitesi üzerinde meydana getirdiği olumsuz tesirlerin $\mathscr{PT}$ periyodik potansiyel ile olan ilişkisi incelenmiştir. $\mathscr{PT}$ periyodik potansiyelin olumsuz etkileri büyük oranda yok ederek kararlı solitonlar elde etmeye yardımcı olduğu gözlenmiştir.

Bölüm 6'da kendine odaklı kübik-kendine odaklı olmayan kuintik ortamda öz-dikleşme etkisine sahip CQNLS denkleminin soliton çözümleri analiz edilmektedir. Kübik nonlineer terimin katsayısı 1, ve kuintik nonlineer terimin katsayısının -1 olması durumunda öz-dikleşme etkisinin solitonların kararlılığını bozamadığı tespit edilmiştir.

Son olarak, bu tezden elde edilen sonuçlar Bölüm 7'de özetlenmiştir.

1. INTRODUCTION

Nonlinear dispersive waves have been the subject of researches for many years, and with the development of some asymptotic methods such as the method of multiple scales, which are used to derive nonlinear wave equations that govern physical phenomena in many fields, they have spread over many areas and made rapid development for more than sixty years. The Korteweg–de Vries (KdV) equation that is used in weakly dispersive and weakly nonlinear systems and the nonlinear Schrödinger (NLS) equation that is used in quasi-monochromatic and weakly nonlinear systems are some of the significant equations derived by the multiple scales method. These universal equations have special solutions, including solitons that appear in all branches of science such as biology [1], solid-state physics [2], Bose-Einstein condensates [3] and nonlinear optics [4].

Solitons are solitary waves that propagate without changing their special structures as a result of the balance between the group velocity dispersion effect and the nonlinear effect. In 1973 Hasegawa and Tappert showed that the nonlinear Schrödinger equation has soliton type solutions [5]. They also discovered that light pulse propagation in optical fibers can be modeled with the NLS equation . Optical solitons provide a great advantage in long-distance communication systems as they can propagate over long distances without being affected by the chromatic and polarization mode dispersion in fiber transmission systems.

In optical fibers, the envelope of the electromagnetic field of the light signal contains the signal information and changes slowly because it has a high-frequency carrier wave. Also, since the refractive index to which the light signal is exposed in the fiber depends on the intensity of the light , this phenomenon is called the Kerr nonlinear effect, the light signal has weak nonlinearity.

In one dimensional (1D) physical systems, weakly nonlinear and dispersive wave packets are governed by the nonlinear Schrödinger equation [6]

$$iu_z + \frac{\beta}{2}u_{xx} + \gamma_1 |u|^2 u = 0, \tag{1.1}$$

where u is the envelope proportional to the electric field, x is the transverse coordinate, z is the distance along the direction of propagation, γ_1 is the coefficient of the cubic (Kerr-type) nonlinear term that depends on intensity, u_{xx} corresponds to diffraction and β is the diffraction coefficient. Diffraction can be thought of as the expansion of a light beam over distance when it passes through air or a crystal. The equivalent of this term, which is called diffraction in optics, in water waves is dispersion.

The nonlinear index coefficient can not always be correctly defined with the usual cubic model [7]. In nonlinear optics, the propagation of the electromagnetic wave in photorefractive materials is described by the cubic-quintic nonlinear Schrödinger (CQNLS) equation [8]. Videlicet, both cubic and quintic nonlinear index variations are considered with two-photon nonlinear absorption in a medium [9]. The CQNLS equation can be written as

$$iu_z + \frac{\beta}{2}u_{xx} + \gamma_1 |u|^2 u + \gamma_2 |u|^4 u = 0, \tag{1.2}$$

where γ_1 is the coefficient of the cubic nonlinear term and γ_2 is the coefficient of the quintic nonlinear term. Different types of media can be defined according to whether γ_1 and γ_2 are positive or negative. The positive sign indicates the nonlinear optical process is self-focusing and the negative sign indicates the nonlinear optical process is self-defocusing. Two different media are examined in this study. These are $\gamma_1 = 1$, $\gamma_2 = 0$ (self-focusing cubic medium), and $\gamma_1 = 1$, $\gamma_2 = -1$ (self-focusing cubic, self-defocusing quintic medium).

Equation (1.2) can be considered together with the complex potential which has parity-time ($\mathscr{P}\mathscr{T}$) symmetry. $\mathscr{P}\mathscr{T}$- symmetric systems may not be isolated, but they are in equilibrium and have completely real energy levels. In an optical waveguide, the real part of the $\mathscr{P}\mathscr{T}$- symmetric potential corresponds to the spatial distribution of the refractive index, and the imaginary part corresponds to the balanced gain-loss relationship.

In this thesis we worked with the following $\mathscr{P}\mathscr{T}-$ symmetric potential:

$$V_{\mathscr{P}\mathscr{T}}(x) = V_0 \cos^2(x) + iW_0 \sin(2x) \tag{1.3}$$

where V_0 and W_0 are the depths of the real and imaginary parts of the potential, respectively.

As a light pulse travels in an optical fiber, the envelope function $u(x,z)$ satisfies the NLS equation (1.1) at the lowest order of approximation. Whereas, if the width of the light pulses is very small, that is, the frequency is high, some linear and nonlinear higher-order effects not modeled in equation (1.1) become prominent. The third-order dispersion (3OD), fourth-order dispersion (4OD), self-steepening and the Raman effect are some of these higher-order effects [6, 10–12]. The CQNLS equation with the self-steepening effect and Raman effect can be written as

$$iu_z + \frac{\beta}{2}u_{xx} + \gamma_1 |u|^2 u + \gamma_2 |u|^4 u + V_{\mathscr{P}\mathscr{T}}(x)u + is\frac{\partial}{\partial x}\left(|u|^2 u\right) + u\tau\frac{\partial}{\partial x}\left(|u|^2\right) = 0, \tag{1.4}$$

where s is the self-steepening coefficient and τ is the Raman coefficent. τ is considered a complex number in most studies ($Re(\tau) = \tau_r$ and $Im(\tau) = \tau_i$). s and τ are inversely proportional to the pulse width. If pulse width much greater than $1ps$ (picosecond), then these coefficients will be very small. In this case Raman effect and self-steepening effect will be very faint. However, these higher-order effects become particularly noticeable for pulses with pulse durations below 100 femtoseconds [13–15]. Therefore, in nonlinear and quantum optics, Eq. (1.4) is a much better choice than Eq. (1.2) when modeling the propagation of ultrashort pulses.

Most of the nonlinear wave equations encountered in all branches of science are non-integrable, in other words, they can not be solved analytically by the inverse scattering transform method. Solitary wave solutions obtained from non-integrable equations have much more complex and interesting structures than solitary wave solutions of classic integrable equations. For example, these solitary waves can be unstable, can be exposed to the critical collapse in multidimensional situations and can be embedded in the continuous spectrum thus they can have distinctive behaviors.

In non-integrable equations, numerical methods are used in important subjects such as calculation of solitary wave solutions, evolution simulation of obtained solutions and calculation of stability spectra of solitary waves. The finite difference method was

very popular for non-integrable wave equations until spectral methods with very high performance were developed in recent years. In this thesis, some spectral methods are utilized to examine the soliton solutions of the NLS equations. These spectral methods are described in detail in Chapter 3.

1.1 Purpose of Thesis

The NLS equation with higher-order effects (1.4) can not be solved by the inverse scattering transform method. Therefore, this equation should be handled with some numerical methods. The aim of this thesis is to find soliton solutions of Eq. (1.4) and to examine the dynamic properties of these solitons to provide the necessary conditions for solitons to be in a stable state. For this purpose, Chapter 3 describes how Eq. (1.4) can be solved by the pseudospectral renormalization method [16]. Also, in Chapters 5 and 6, the effects of the self-steepening term and the $\mathscr{PT}$- symmetric periodic potential on the stability of solitons obtained from the NLS and CQNLS equations are examined.

1.2 Literature Review

In the linear wave phenomenon, waves undergo dispersion, so over time the width of the wave increases and its amplitude decreases. In 1834, Scott Russell noticed a wave of water rolling forward in a canal near Edinburgh, without change in speed and form. Russell named this phenomenon, which he observed for the first time, the Wave of Translation [17]. In 1895, Diederik Korteweg and Gustav de Vries realized that to occur the phenomenon of the Wave of Translation, which could not be elucidated by the linear wave theory and which was a matter of curiosity for a long time, the dispersion that causes the decay of the wave had to be balanced with the nonlinear effects in the medium that cause the wave to steepen. Then, they derived the Korteweg–de Vries (KdV) equation to model solitary waves that do not deform when rolled forward, as in the Wave of Translation phenomenon. [18]. In 1965, Zabusky and Kruskal investigated the solitary wave solutions of the KdV equation numerically and discovered that the collisions of these solitary waves with each other are elastic [19]. In 1967, Gardner, et al. solved the KdV equation analytically with the inverse scattering transform method they developed then this method was used to obtain the analytical solution of many

nonlinear equations such as the sine-Gordon equation, the Kadomtsev–Petviashvili (KP) equation and the NLS equation. These equations that can be solved by the inverse scattering transform method are called integrable equations.

Benney and Newell derived the nonlinear Schrödinger (NLS) equation in 1967 [20], and Zakharov soon used it in his work on deep water waves [21]. In 1973 Hasegawa and Tappert solved the nonlinear Schrödinger equation and found solutions for solitary waves, i.e. solitons [5]. They also showed that the NLS equation governs the light pulse propagation in optical fibers and it was realized that soliton propagation could potentially be used to great advantage in long-distance systems. Then, research on optical solitons has intensified and its various effects are much better understood.

When the group velocity of an optical pulse depends on the density, the self-steepening effect occurs. In 1967, De Martini et al. examined the causes and consequences of the self-steepening effect [22]. In 1978, Kaup and Newell showed that the NLS equation which has the self-steepening term but no self-phase modulation is integrable [23]. They used the inverse scattering method in their work. But later on, soliton solutions were also obtained by the Hirota method [24] and the Darboux transformation [25]. Moses et al. stated that the ability to shape pulses through self-steepening in the absence of self-phase modulation may find simple applications in studies of light-matter interactions [26]. Anderson and Lisak showed that self-steepening plays an important role for short-pulse propagation in long optical waveguides [27]. Thuy et al. investigated the influence of self-steepening and higher dispersion effects on the propagation characteristics of solitons in fiber [12]. Abdel Kader et al. examined the existence and stability properties of nonlinearly chirped solitary waves on a continuous wave background in nonlinear metamaterials with higher-order effects such as pseudo-quintic nonlinearity and self-steepening effect [28].

In 1976, Petviashvili developed a spectral numerical method to solve the Kadomtsev-Petviashvili equation [29]. Later, this method was extended many times to find localized solutions in various systems, including NLS equations [30–35]. In 2005, Ablowitz and Musslimani developed the spectral renormalization (SR) method [16]. Unlike other Petviashvili methods, the SR method can find localized solutions in nonlinear waveguides which has higher-order nonlinearities with different homogeneities. However, if the system does not have homogeneous nonlinearity as in

saturable nonlinearity, another root finding method should be used together with the SR method. In 2014, Antar derived the pseudospectral renormalization (PSR) method from the SR method, which can directly reach the result even in inhomogeneous systems without the need for another method [36].

In materials with high nonlinear coefficients such as semiconductor doped glasses, organic polymers, the optically induced refractive-index change becomes saturated due to higher field strength. In reference [37], the soliton solutions of the generalized NLS equation modeling soliton propagation in saturable nonlinear materials were investigated both numerically and analytically, and the stability analysis of the obtained solutions was performed.

In reference [38], the preliminary steps of supercontinuum generation in photonic crystal fibers pumped with femtosecond pulses at various wavelengths in the anomalous dispersion regime were examined both experimentally and numerically.

In 1998, Bender and Boettcher discovered $\mathscr{P}\mathscr{T}$- symmetric quantum systems, postulating the idea that Hermitian Hamiltonians can be extended to non-Hermitian Hamiltonians [39]. After that, $\mathscr{P}\mathscr{T}$- symmetric systems became the subject of research in many fields such as microwave cavities [40], electronic circuits [41], lasers [42], chaos and noise [43] and optics [44,45]. In 2008, Musslimani et al. studied the existence, stability and propagation dynamics of solitons in $\mathscr{P}\mathscr{T}$- symmetric lattices [46]. Subsequently, many studies have been done on $\mathscr{P}\mathscr{T}$ solitons [47,48]. In recent years, $\mathscr{P}\mathscr{T}$ solitons in cubic-quintic nonlinear systems have also been examined [8,49,50].

The CQNLS equation with the Raman term is also called the Kundu-Eckhaus (KE) equation. Analytical solutions of the KE equation are examined in [51, 52] . Also in [53], the self-localized solutions of the KE equations are studied numerically using the SR method.

1.3 Hypothesis

In fiber optic systems, the width of the optical pulses is reduced to increase the bandwidth and communication speed. As a result, some higher-order effects occur. Many studies have been done on NLS equations with higher-order effects in the

literature. These higher-order effects are known to adversely affect the existence and stability of solitons. In this study, it is claimed that these negative effects caused by higher-order effects on solitons can be avoided by $\mathscr{PT}$- symmetric potentials.

2. OPTICAL SOLITONS

Optical solitons are solitary waves that occur as a result of the balance between the group velocity dispersion effect and the nonlinear effect caused by the change in refractive index due to the Kerr effect. Soliton generation and analysis in optics is a pretty popular and modern research topic, as optical solitons have a wide range of applications, such as optical communication technology, pulse compression in ultrafast optics and all-optical switching. Particularly, the propagation of optical solitons in fiber optic communication systems is an area of great interest to researchers.

Optical solitons can propagate through long distances in fiber transmission systems without being affected by chromatic and polarization mode dispersion. Since their natural structure is preserved, they can be used as natural optical bits of information in fiber optic systems. The propagation of light in the single-mode fiber is governed by the nonlinear Schrödinger (NLS) equation (1.1). Figure 2.1 shows that the structure of the fundamental soliton obtained from Eq. (1.1) is conserved during its spatial evolution.

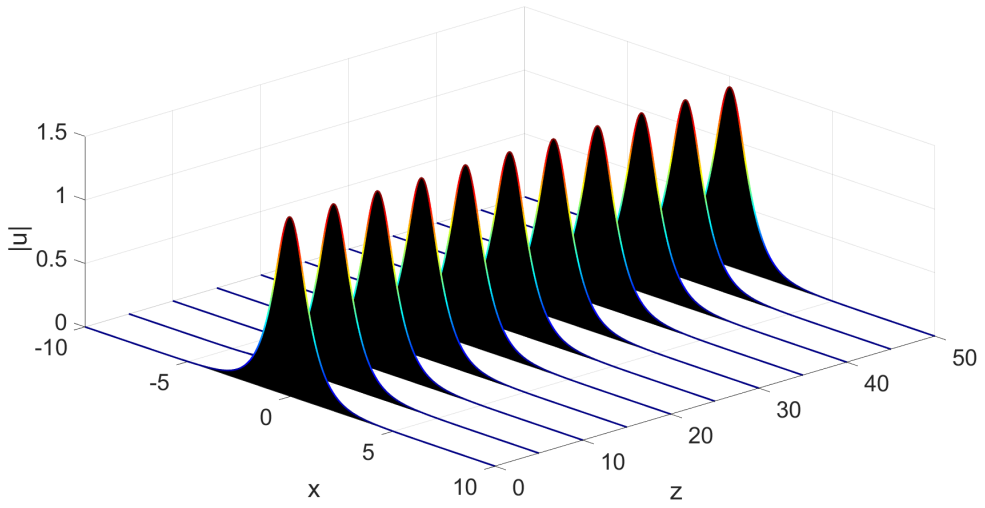

Figure 2.1 : The evolution of the numerically obtained fundamental soliton solution of Eq. (1.1) when $\beta = 1$ and $\gamma_1 = 1$.

Higher-order solitons are solitons whose energies are equal to the energies of the fundamental solitons multiplied by the square of an integer (4,9,16, etc.). Therefore, higher-order solitons are useful for producing short pulses of light. The temporal shape of higher-order solitons is not constant but shows a periodic behavior during propagation. These pulses repeat their shape with a period of p_0:

$$p_0 = \frac{\pi}{2} L_0, \tag{2.1}$$

where

$$L_0 = \frac{f_0^2}{|\beta|}, \tag{2.2}$$

f_0 is related to the pulse duration. Besides exhibiting periodic behavior, higher-order solitons can be separated into fundamental solitons in some cases by effects such as self-steepening, higher-order dispersion, and Raman scattering. This phenomenon plays an important role in the supercontinuum generation process in photonic crystal fibers [38].

Higher-order soliton solutions of the NLS equation can be found with the initial amplitude

$$u(x, z = 0) = Nu(x), \tag{2.3}$$

where $u(x)$ is the fundamental soliton solution of the NLS equation and N is an integer ($N = 2, 3, 4, 5...$). The evolution of the numerically obtained 2-soliton and 3-soliton solutions of the NLS equation is shown in Figures 2.2 and 2.3, respectively.

2.1 Solitons in Optical Lattices

Optical lattices are spatially periodic polarization patterns obtained by the interference of counter-propagating laser beams. In optical lattices, some properties of solitons can be controlled by varying the lattice depth and period. In this thesis, $\mathscr{P}\mathscr{T}$- symmetric lattices were used.

2.1.1 $\mathscr{P}\mathscr{T}$- Symmetry

In both classical and quantum physical systems, the behavior and properties of the system are characterized by a quantity named the Hamiltonian. Previously, in quantum physics, Hamiltons were divided into two main groups according to whether they

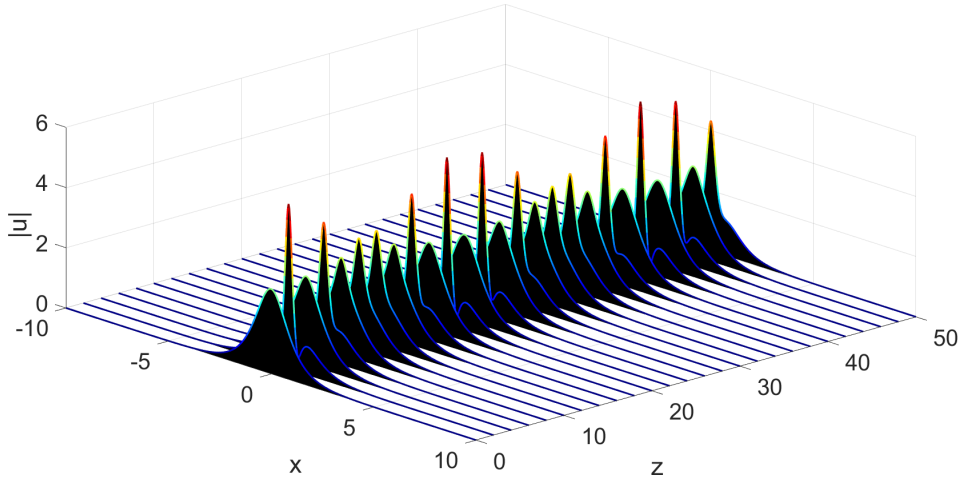

Figure 2.2 : The evolution of the numerically obtained 2-soliton solution of Eq. (1.1) when $\beta = 1$ and $\gamma_1 = 1$.

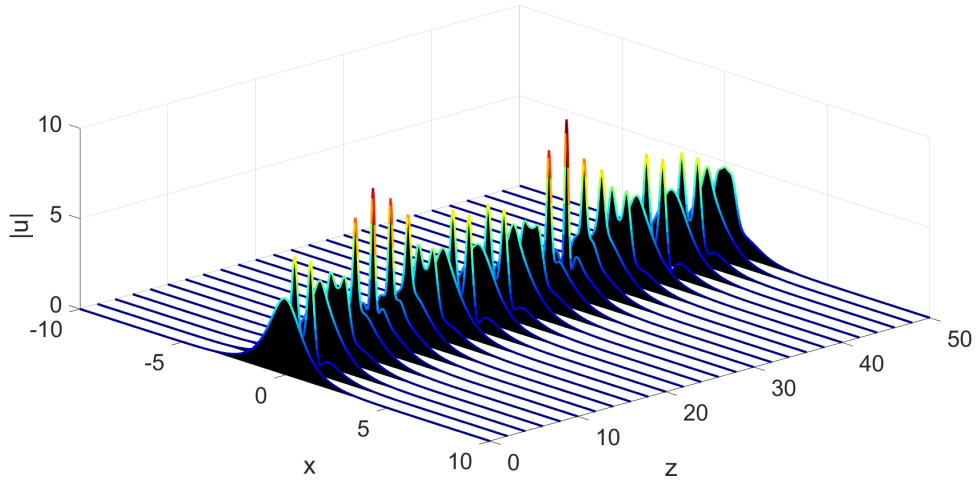

Figure 2.3 : The evolution of the numerically obtained 3-soliton solution of Eq. (1.1) when $\beta = 1$ and $\gamma_1 = 1$.

were Hermitian or not. Hermitian Hamiltonians specify the character of idealized and isolated systems in equilibrium whose energy levels are real and whose total energy and probability do not change. On the other hand, non-Hermitian Hamiltonians specify the character of systems in contact with the environment. Such non-isolated systems can exchange energy with their surroundings, therefore they are not in equilibrium, the total energy and probability are not constant, and the energy levels are represented by complex numbers.

In 1998, Bender and Boettcher discovered $\mathscr{P}\mathscr{T}$- symmetric quantum systems, postulating the idea that Hermitian Hamiltonians can be extended to non-Hermitian Hamiltonians [39]. These systems are called $\mathscr{P}\mathscr{T}$- symmetric because they are invariant under the combined operation of space reflection (represented by parity operator $\widehat{\mathscr{P}}$)

$$\widehat{\mathscr{P}}: \widehat{p} \to -\widehat{p},\ \widehat{x} \to -\widehat{x}, \qquad \mathscr{P}(a\psi + b\phi)(\boldsymbol{x}) = a\psi(-\boldsymbol{x}) + b\phi(-\boldsymbol{x}), \tag{2.4}$$

and reversing the arrow of time (represented by $\widehat{\mathscr{T}}$)

$$\widehat{\mathscr{T}}: \widehat{p} \to -\widehat{p},\ \widehat{x} \to \widehat{x},\ i \to -i, \quad \mathscr{T}(a\psi + b\phi)(\boldsymbol{x}) = a^*\psi^*(\boldsymbol{x}) + b^*\phi^*(\boldsymbol{x}), \tag{2.5}$$

where $\widehat{x}$ and $\widehat{p}$ are position and momentum operators respectively. $\mathscr{P}\mathscr{T}$- symmetric Hamiltonians are a special kind of Hamiltonian at a level between the Hermitian and non-hermitian Hamiltonians known in classic quantum physics. Unlike Hermitian systems, $\mathscr{P}\mathscr{T}$- symmetric systems are not isolated but have characteristics of Hermitian systems. Because, these systems have a special relationship with their environment, the gain from the surroundings and the loss to the surroundings are in perfect balance. Thus, although $\mathscr{P}\mathscr{T}$- symmetric systems are not isolated, they are in equilibrium and have completely real energy levels [54].

2.1.2 $\mathscr{P}\mathscr{T}$ periodic potentials

In general, a Hamiltonian can be considered as follows

$$\widehat{H} = \widehat{T} + \widehat{V} = \frac{\widehat{p}^2}{2m} + \widehat{V}(\widehat{x}), \tag{2.6}$$

where m is mass and $\widehat{V}$ is the complex potential. For a Hamiltonian to be $\mathscr{P}\mathscr{T}$-symmetric, $\widehat{\mathscr{P}}\widehat{\mathscr{T}}\widehat{H} = \widehat{H}\widehat{\mathscr{P}}\widehat{\mathscr{T}}$, it must have the same eigenstates as the $\mathscr{P}\mathscr{T}$ operator. For the commutative property to be provided,

$$\begin{aligned}(\mathscr{P}\mathscr{T}H)(f(\boldsymbol{x},t)) &= (\mathscr{P}\mathscr{T})\left(\frac{p^2}{2m}f(\boldsymbol{x},t) + V(\boldsymbol{x})f(\boldsymbol{x},t)\right) \\ &= \mathscr{P}\left(\frac{(-p)^2}{2m}f^*(\boldsymbol{x},t) + V^*(\boldsymbol{x})f^*(\boldsymbol{x},t)\right) \\ &= \frac{p^2}{2m}f^*(-\boldsymbol{x},t) + V^*(-\boldsymbol{x})f^*(-\boldsymbol{x},t)\end{aligned} \tag{2.7}$$

and

$$
\begin{aligned}
(H\mathscr{P}\mathscr{T})(f(\boldsymbol{x},t)) &= (H\mathscr{P})\,(f^*(\boldsymbol{x},t)) \\
&= H\,(f^*(-\boldsymbol{x},t)) \\
&= \frac{p^2}{2m} f^*(-\boldsymbol{x},t) + V(\boldsymbol{x}) f^*(-\boldsymbol{x},t)
\end{aligned}
\tag{2.8}
$$

must be equal to each other. In that case, $V(\boldsymbol{x}) = V^*(-\boldsymbol{x})$ is a necessary condition for a Hamiltonian to be $\mathscr{P}\mathscr{T}$- symmetric, but not a sufficient condition. This means that the real part (for the spatial distribution of the refractive index) of the potential must be an even function and the imaginary part (for the balanced gain and loss) must be an odd function.

Consider the complex potential:

$$
V_{\mathscr{P}\mathscr{T}}(x) = V_{\mathrm{R}}(x) + i\varepsilon V_{\mathrm{I}}(x), \tag{2.9}
$$

where V_{R} and V_{I} are the symmetric and antisymmetric parts of V, respectively. When ε is equal to zero, the Hamiltonian becomes Hermitian. Furthermore, as long as the ε is less than a certain threshold value, the Hamiltonian has a completely real spectrum and above this threshold value, imaginary eigenvalues occur in the spectrum. This phenomenon is called $\mathscr{P}\mathscr{T}$- symmetry breaking.

In this thesis, we examined optical beam propagation in $\mathscr{P}\mathscr{T}$- symmetric complex potentials and used the following periodic potential:

$$
V_{\mathscr{P}\mathscr{T}}(x) = V(x) + iW(x) = V_0 \cos^2(x) + iW_0 \sin(2x), \tag{2.10}
$$

where V_0 and W_0 are the depths of the real and imaginary parts of the potential, respectively. In figure 2.4, it is seen that the real part of the potential (refractive-index profile) is even and the imaginary part (gain/loss distribution) is odd.

2.2 Higher-Order Effects on Optical Solitons

The propagation of the light pulse in optical fibers is mathematically modeled by the NLS equation (1.1), and the soliton solution $u(x,z)$ satisfies the NLS equation at the lowest order of approximation [6]. However, when the light pulse is too short, the classical NLS equation may be insufficient to model the physical system. Because if the light pulse is short, often some higher-order effects need to be taken into account. It can be said that the third-order dispersion, self-steepening (or nonlinear dispersion) and

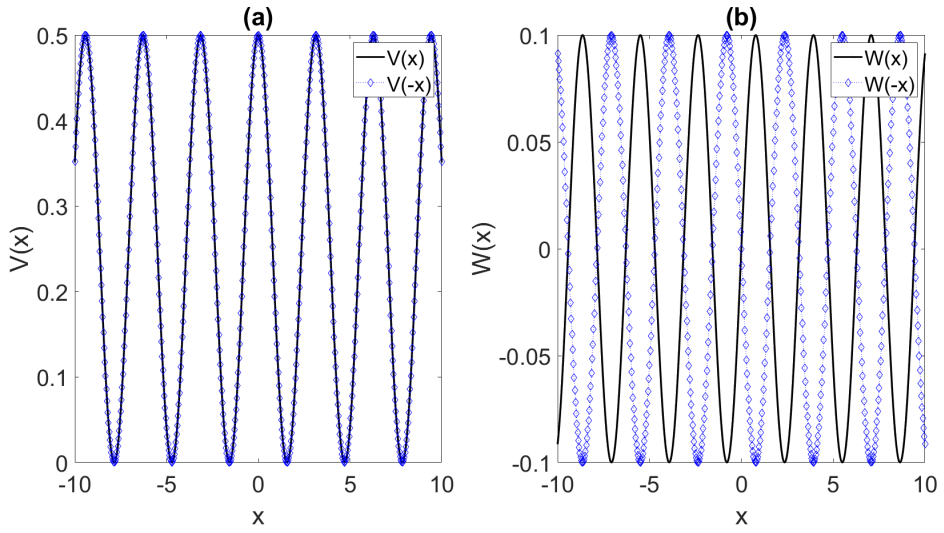

Figure 2.4 : (a) Real part, (b) Imaginary part of the potential in equation (2.10) when $V_0 = 0.5$ and $W_0 = 0.1$.

the Raman effect are the most significant higher-order effects. The CQNLS equation with the self-steepening effect and Raman effect can be written as (see [10] and [11])

$$iu_z + \frac{\beta}{2}u_{xx} + \gamma_1|u|^2u + \gamma_2|u|^4u + is\frac{\partial}{\partial x}\left(|u|^2u\right) + u\tau\frac{\partial}{\partial x}\left(|u|^2\right) = 0, \qquad \textbf{(2.11)}$$

where u is the envelope function which is proportional to the electric field, z is the propagation direction of optical pulse, γ_1 and γ_2 are the coefficients of the cubic and quntic nonlinear terms, respectively, which depend on intensity, u_{xx} corresponds to the diffraction term and β is the diffraction coefficient.

s and τ are the self-steepening and Raman coefficients, respectively, and they are inversely proportional to the pulse width. This relationship is clearly seen from the formulas:

$$s = \frac{1}{\omega_0 T_0}, \quad \tau = \frac{T_R}{T_0}, \qquad \textbf{(2.12)}$$

where T_R is the Raman coefficient which is related to the slope of the Raman gain spectrum, T_0 is the pulse width, $\omega_0 = \omega(k_0)$, and k_0 is the dominant wavenumber of the wave packet, $\omega = \omega(k)$ is the linear dispersion relation for Fourier waves $e^{i(kx-\omega t)}$.

If the pulse width is much greater than $1ps$ (picosecond), then these coefficients will be too small. In this case Raman effect and self-steepening effect will be very faint. But for femtosecond pulses, these coefficients may be remarkable. Assuming the pulse width is around $30fs$ and T_R is around $3fs$ at wavelength λ near $1.55\mu m$, the s and τ coefficients correspond to approximately 0.03 and 0.1, respectively [6, 11]. These

coefficients have significant values that can not be neglected. Therefore equation (1.1) should be considered together with the higher order terms mentioned.

It is known that, equation (1.1) can be solved analytically by the inverse scattering transform method [55]. Thus, it is called an integrable equation. However the NLS equation with higher order effects is not integrable. In Chapters 5 and 6, solutions and stability analyses of the NLS and CQNLS equations with the self-steepening and the $\mathscr{P}\mathscr{T}$ periodic potential are numerically investigated.

2.2.1 Self-Steepening Effect

The NLS equation under the self-steepening effect can be written as follows:

$$iu_z + \frac{\beta}{2}u_{xx} + \gamma_1|u|^2u + is\frac{\partial}{\partial x}\left(|u|^2u\right) = 0, \tag{2.13}$$

where $\left(|u|^2u\right)_x$ is the self-steepening term of the NLS equation. The self-steepening term in equation (2.13) causes the optical pulse to shift in position as it travels in the z direction. Position shift occurs by sr^2z amount, here r is the soliton amplitude. As the soliton moves in the z direction, the position shift increases linearly. This is the most important and well-known effect of the self-steepening term.

The self-steepening effect occurs, when the group velocity of an optical pulse depends on the density. In such a case, since the group velocity is density dependent, the peak of an optical pulse moves slower than its wings. Therefore, the self-steepening causes the top of an optical pulse to become steeper towards the trailing edge and causes an optical pulse to become asymmetric [56]. In other words, it causes an optical shock at the trailing edge, especially in the absence of the GVD effect [12]. In Figure 2.5, β is equal to 0, and the propagation of the optical pulse under the self-steepening and self-phase modulation effect is shown, the *sech* soliton is taken as the initial condition. In the figure, it is seen that the self-steepening produces mentioned optical shock within a short distance when the optical soliton propagates.

The second order dispersion dampens the effects of the self-steepening to a remarkable amount. In Figure 2.6, β has been changed to 1. It is clearly seen that the GVD absorbs the shock effect. However, the self-steepening still shows its effect by causing a shift in the position of the pulse, making the pulse asymmetric and dividing the pulse into sub-pulses. In conclusion, although second order dispersion reduces the effects of the

self-steepening by a notable amount, self-steepening continues to severely affect the stability of the soliton.

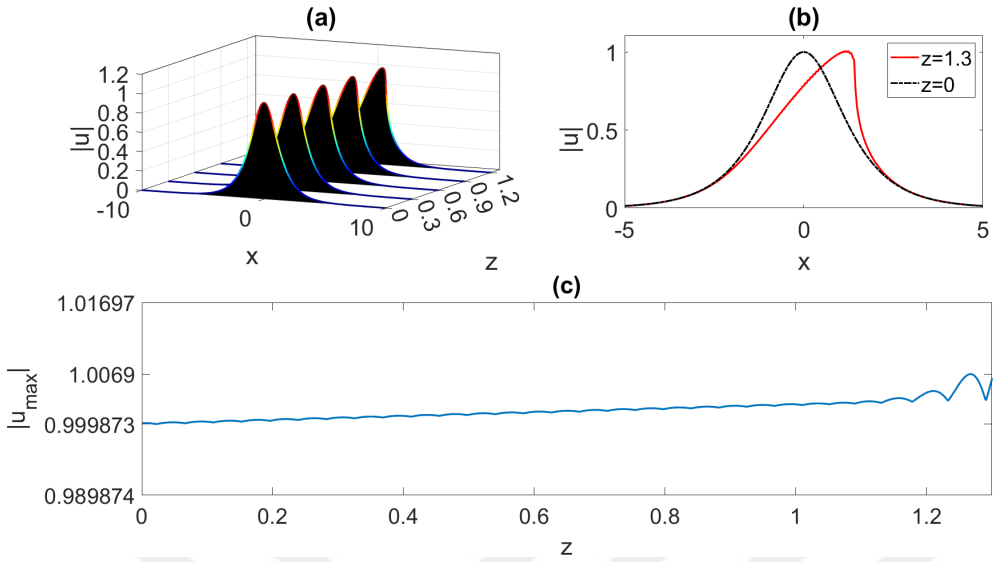

Figure 2.5 : Influence of self-steepening and self-phase modulation effect on the propagation characteristic of ultrashort pulses ($\beta = 0$, $s = 0.3$), (a) Nonlinear evolution of the soliton, (b) Optical pulses at $z = 0$ and $z = 1.3$, (c) Maximum amplitude as a function of the propagation distance z.

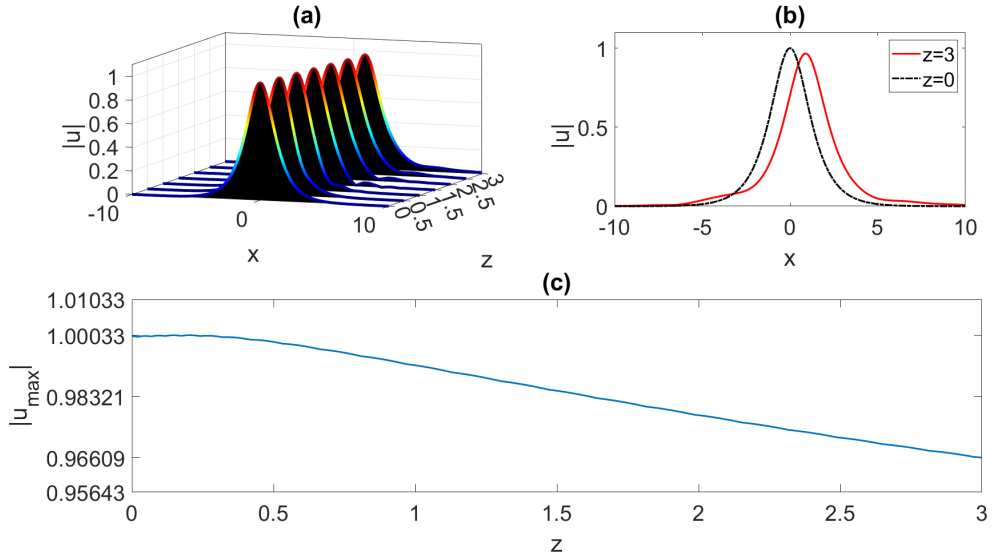

Figure 2.6 : (a) Nonlinear evolution of the *sech* pulse ($\beta = 1$, $s = 0.3$), (b) Optical pulses at $z = 0$ and $z = 3$, (c) Maximum amplitude as a function of the propagation distance z.

3. NUMERICAL METHODS

Numerical methods are very often used in solving nonlinear equations. Many important phenomena in physics and mathematics were discovered by numerical methods. Elastic collision of KdV solitons and fractal scattering in solitary wave interactions are a few of them [19].

Many nonlinear equations can not be solved analytically. They are called non-integrable equations. Since the equations examined in this thesis are also non-integrable, numerical methods were used in this study as well.

In this chapter, some numerical methods used for different purposes are explained. These are pseudospectral renormalization method, split-step method and Fourier collocation method are used for computation of solitary wave solutions, evolution simulation and computation of linear-stability spectra of solitary waves, respectively. These methods give very accurate results for the equations studied in this thesis. Accuracies, numerical stability, convergence conditions and convergence speeds of these three methods are explained in detail in reference [6].

3.1 Pseudospectral Renormalization Method

There are some numerical methods for calculating solitary waves such as shooting method, squared-operator iteration methods [57], accelerated imaginary-time evolution method [58, 59], Newton conjugate-gradient methods [60], Petviashvili method [29] etc.

The Petviashvili method was first used to obtain localized solutions in two-dimensional KdV equation. This method is based on transforming to Fourier space and the fixed-point iteration with the improvement of determining a convergence factor. Later, this method was extended to find localized solutions in various systems [30–34]. One of the most important methods derived from the Petviashvili method is the spectral renormalization method [16]. With the spectral renormalization method, localized

solutions in nonlinear waveguides can be calculated. Also, this method can be used in various fields such as fluid dynamics and Bose–Einstein condensation. The spectral renormalization method is easy to implement and usually converges fairly quickly. One of the most important features that distinguishes it from other Petviashvili methods is that it can be applied to equations which has higher order nonlinearities with different homogeneities such as cubic-quintic equations. On the other hand, when the system lacks any homogeneity, as in saturable nonlinearity, the convergence factor can not be found explicitly by the spectral renormalization method. In order to find the convergence factor, a root finding method should be used. In reference [36], the pseudospectral renormalization method is derived from the spectral renormalization method so that the convergence factor can be found explicitly even in the lacks of homogeneity, as in the saturable case .

In this section, the cubic-quintic NLS equation with the external potential, Raman effect and self-steepening effect is solved using the pseudospectral renormalization (PSR) method. The governing equation:

$$iu_z + \frac{\beta}{2}u_{xx} + \gamma_1 |u|^2 u + \gamma_2 |u|^4 u + V_{\mathscr{P}\mathscr{T}}(x)u + is\frac{\partial}{\partial x}\left(|u|^2 u\right) + \tau u\frac{\partial}{\partial x}\left(|u|^2\right) = 0, \quad \textbf{(3.1)}$$

where τ is a complex number. $Re(\tau) = \tau_r$ and $Im(\tau) = \tau_i$. The self-steepening term can be written as $(is)\,u\frac{\partial}{\partial x}\left(|u|^2\right) + is|u|^2\frac{\partial}{\partial x}u$. Thus, equation (3.1) can be written more clearly as in equation (3.2):

$$iu_z + \frac{\beta}{2}u_{xx} + \gamma_1 |u|^2 u + \gamma_2 |u|^4 u + V_{\mathscr{P}\mathscr{T}}(x)u + (\tau_r + is_1)\,u\frac{\partial}{\partial x}\left(|u|^2\right) + is|u|^2\frac{\partial}{\partial x}u = 0, \quad \textbf{(3.2)}$$

here, s_1 corresponds to $\tau_i + s$.

If the ansatz $u(x,z) = f(x)e^{i\mu z}$ is used, $f(x)$ is a complex valued function and μ is the propagation constant (eigenvalue), the following expressions are obtained:

$$\begin{aligned} u_z(x,z) &= i\mu f e^{i\mu z}, \\ u_{xx}(x,z) &= f_{xx}e^{i\mu z}, \\ |u(x,z)|^2 &= f e^{i\mu z}\cdot f e^{-i\mu z} = |f|^2, \\ |u(x,z)|^4 &= |f|^4. \end{aligned} \quad \textbf{(3.3)}$$

Substituting the expressions in equation (3.3) into equation (3.2) gives the following equation:

$$\begin{aligned} &-\mu f e^{i\mu z} + \frac{\beta}{2} f_{xx} e^{i\mu z} + \gamma_1 |f|^2 f e^{i\mu z} + \gamma_2 |f|^4 f e^{i\mu z} + V f e^{i\mu z} \\ &+ f e^{i\mu z} (\tau_r + i s_1) \frac{\partial}{\partial x} \left(|f|^2 \right) + i s |f|^2 f_x e^{i\mu z} = 0. \end{aligned} \tag{3.4}$$

Equation (3.4) is simplified by discarding the exponential terms:

$$-\mu f + \frac{\beta}{2} f_{xx} + \gamma_1 |f|^2 f + \gamma_2 |f|^4 f + V f + f (\tau_r + i s_1) \frac{\partial}{\partial x} \left(|f|^2 \right) + i s |f|^2 f_x = 0. \tag{3.5}$$

The Fourier transform and the inverse Fourier transform of the differential terms in equation (3.5) are taken, respectively, and equation (3.6) is obtained. The resulting equation no longer contains expressions with differentials.

The Fourier transform of f is shown as $\mathscr{F}(f) = \hat{f}$, the inverse Fourier transform of $\hat{f}$ is shown as $\mathscr{F}^{-1}(\hat{f})$, and obviously $\mathscr{F}^{-1}(\hat{f}) = \mathscr{F}^{-1}(\mathscr{F}(f)) = f$.

$$\begin{aligned} &-\mu f - \frac{\beta}{2} \mathscr{F}^{-1} \left\{ k^2 \hat{f} \right\} + \gamma_1 |f|^2 f + \gamma_2 |f|^4 f + V f \\ &+ f (\tau_r + i s_1) \mathscr{F}^{-1} \left\{ ik \mathscr{F} \left\{ |f|^2 \right\} \right\} + i s |f|^2 \mathscr{F}^{-1} \left\{ ik \hat{f} \right\} = 0, \end{aligned} \tag{3.6}$$

here, k is the Fourier variable.

The Fourier transform of equation (3.6) is taken and equation (3.7) is obtained:

$$\begin{aligned} &-\mu \hat{f} - \frac{\beta}{2} k^2 \hat{f} + \gamma_1 \mathscr{F} \left\{ |f|^2 f \right\} + \gamma_2 \mathscr{F} \left\{ |f|^4 f \right\} + \mathscr{F} \{ V f \} \\ &+ \mathscr{F} \left\{ f (\tau_r + i s_1) \mathscr{F}^{-1} \left\{ ik \mathscr{F} \left\{ |f|^2 \right\} \right\} \right\} + \mathscr{F} \left\{ i s |f|^2 \mathscr{F}^{-1} \left\{ ik \hat{f} \right\} \right\} = 0. \end{aligned} \tag{3.7}$$

Equation (3.7) is indexed and $\hat{f}$ can be tried to be found with the fixed point iteration using the formula below:

$$\hat{f}_{n+1} = \frac{\begin{pmatrix} \gamma_1 \mathscr{F} \left\{ |f_n|^2 f_n \right\} + \gamma_2 \mathscr{F} \left\{ |f_n|^4 f_n \right\} + \mathscr{F} \{ V(x) f_n \} \\ + \mathscr{F} \left\{ f_n (\tau_r + i s_1) \mathscr{F}^{-1} \left\{ ik \mathscr{F} \left\{ |f_n|^2 \right\} \right\} \right\} + \mathscr{F} \left\{ i s |f_n|^2 \mathscr{F}^{-1} \left\{ ik \hat{f}_n \right\} \right\} \end{pmatrix}}{\mu + \frac{\beta}{2} k^2}. \tag{3.8}$$

But the iteration only converges to the trivial solution. That's $u(x,z) = 0$ and this is definitely not what we're looking for. A new variable must be defined in order to achieve the desired solution.

Let's take $f(x) = \lambda w(x)$ and $\hat{f}(x) = \lambda \hat{w}(x)$. Here $\lambda \in R^+$ and it's called renormalization constant.

Substituting the new variable in equation (3.6), we get equation (3.9):

$$\begin{aligned}&-\mu\lambda w-\frac{\beta}{2}\lambda\mathscr{F}^{-1}\left\{k^2\hat{w}\right\}+\gamma_1|\lambda|^2\lambda|w|^2w+\gamma_2|\lambda|^4\lambda|w|^4w+V\lambda w\\&+\lambda|\lambda|^2w(\tau_r+is_1)\mathscr{F}^{-1}\left\{ik\mathscr{F}\left\{|w|^2\right\}\right\}+is|w|^2\mathscr{F}^{-1}\left\{ik\hat{w}\right\}\lambda|\lambda|^2=0.\end{aligned}\tag{3.9}$$

Some simplifications are made and equation (3.10) is obtained:

$$\begin{aligned}&-\mu w-\frac{\beta}{2}\mathscr{F}^{-1}\left\{k^2\hat{w}\right\}+V(x)w\\&+|\lambda|^2\left(\gamma_1|w|^2w+w(\tau_r+is_1)\mathscr{F}^{-1}\left\{ik\mathscr{F}\left\{|w|^2\right\}\right\}+is|w|^2\mathscr{F}^{-1}\left\{ik\hat{w}\right\}\right)\\&+|\lambda|^4\gamma_2|w|^4w=0.\end{aligned}\tag{3.10}$$

Equation (3.10) is multiplied by $\hat{w}^*$, $\hat{w}^*$ is the conjugate of $\hat{w}$, and then integrated:

$$\begin{aligned}&\int_{-\infty}^{\infty}\Big[-\mu ww^*-\frac{\beta}{2}w^*\mathscr{F}^{-1}\left\{k^2\hat{w}\right\}+V(x)ww^*\Big]dx\\&+|\lambda|^2\int_{-\infty}^{\infty}w^*\Big[\gamma_1|w|^2w+w(\tau_r+is_1)\mathscr{F}^{-1}\left\{ik\mathscr{F}\left\{|w|^2\right\}\right\}+is|w|^2\mathscr{F}^{-1}\left\{ik\hat{w}\right\}\Big]dx\\&+|\lambda|^4\int_{-\infty}^{\infty}w^*\gamma_2|w|^4wdx=0.\end{aligned}\tag{3.11}$$

Equation (3.11) can be thought of as a fourth order polynomial in terms of λ. It's known that, if $P(\lambda)$ is equal to $a\lambda^4+b\lambda^2+c$ then λ is found by the formula:

$$\lambda_{1,2}=\pm\sqrt{\frac{-b\pm\sqrt{b^2-4ac}}{2a}},\tag{3.12}$$

where

$$\begin{aligned}a&=\int_{-\infty}^{\infty}\gamma_2|w|^6dx,\\b&=\int_{-\infty}^{\infty}w^*\Big[\gamma_1|w|^2w+w(\tau_r+is_1)\mathscr{F}^{-1}\left\{ik\mathscr{F}\left\{|w|^2\right\}\right\}+is|w|^2\mathscr{F}^{-1}\left\{ik\hat{w}\right\}\Big]dx,\\c&=\int_{-\infty}^{\infty}\Big[-\mu ww^*-\frac{\beta}{2}w^*\mathscr{F}^{-1}\left\{k^2\hat{w}\right\}+V(x)ww^*\Big]dx.\end{aligned}\tag{3.13}$$

Now we need to create an iteration formula to find w. So let's go back to equation (3.10). Firstly the Fourier transform of equation (3.10) is taken. Then, $+r\hat{w}-r\hat{w}$ is added to the equation so that μ does not come to the denominator in the iteration formula to be created. Thus, the possibility of the denominator being zero is eliminated.

After the operations are performed, the following equation is obtained:

$$\begin{aligned}&(-\mu+r)\,\hat{w}-\hat{w}\left(r+\frac{\beta}{2}k^2\right)\\&+\mathscr{F}\{V(x)w\}\\&+|\lambda|^2\mathscr{F}\left\{\gamma_1|w|^2w+w\,(\tau_r+is_1)\,\mathscr{F}^{-1}\left\{ik\mathscr{F}\left\{|w|^2\right\}\right\}+is|w|^2\mathscr{F}^{-1}\left\{ik\hat{w}\right\}\right\}\\&+|\lambda|^4\mathscr{F}\left\{\gamma_2|w|^4w\right\}=0.\end{aligned} \tag{3.14}$$

Let's index equation (3.14) and call the
$\mathscr{F}\{V(x)w_n\}+|\lambda_n|^2\mathscr{F}\left\{\gamma_1|w_n|^2w_n+w_n\,(\tau_r+is_1)\,\mathscr{F}^{-1}\left\{ik\mathscr{F}\left\{|w_n|^2\right\}\right\}+is|w_n|^2\mathscr{F}^{-1}\left\{ik\hat{w}_n\right\}\right\}$
$+|\lambda_n|^4\mathscr{F}\left\{\gamma_2|w_n|^4w_n\right\}$
term in equation (3.14) as A_n. Fixed point iteration can now be applied. Thus,

$$\hat{w}_{n+1}=\frac{(-\mu+r)\hat{w}_n+A_n}{r+\frac{\beta}{2}k^2}. \tag{3.15}$$

In this iteration, $w_0=e^{-x^2}$ can be chosen as the initial condition. Then λ_0 is found using equation (3.12) and $\hat{f}(x)$ is obtained from the $\hat{f}(x)=\lambda\hat{w}(x)$. The error is examined by substituting the values in equation (3.6). The iteration continues until the error reaches the desired level. In this thesis, when the error reached the order of 10^{-10}, we stopped the iteration and showed the results.

3.2 Split-Step Method

The split-step method is one of the spectral methods used to simulate the evolution of the nonlinear wave equations.

Evolution simulation is an important tool to see how a nonlinear wave system behaves. Heretofore, it has made enormous contributions to the discovery of previously unrecognized phenomena in physical systems. For example, the existence of solitons was discovered by numerical simulation of the KdV equation using the finite difference method [19].

Before spectral methods were developed, the finite difference methods was pretty popular for evolution simulation. But finite difference methods do not have high accuracy. Therefore, after the development of spectral methods, they are preferred more than finite difference methods. The spatial accuracy of these spectral methods is spectral and have higher accuracy than finite difference methods.

There are many spectral methods. The pseudospectral method [61–64], the integrating-factor method [63–65] and the split-step method [64, 66–68] are some of them. In this study, the split-step method was utilized for evolution simulation.

When the split-step method is applied, the evolution equation is split into some pieces; then, they are integrated respectively. Using these separate integration parts, the numerical solution in the next step is obtained.

3.2.1 Split-step method for linear equations

This section will show how the split-step method is applied to linear PDEs. A linear PDE can be written as follows

$$\psi_z = (L_1 + L_2)\psi, \tag{3.16}$$

where L_1 and L_2 are two linear operators independent of z. The exact solution of Eq. (3.16) at $z = h$ is

$$\psi(x,h) = e^{h(L_1+L_2)}\psi(x,0), \tag{3.17}$$

here h is the step size in z-direction. Eq. (3.16) splits into two equations

$$\begin{aligned} \psi_z &= L_1\psi, \\ \psi_z &= L_2\psi. \end{aligned} \tag{3.18}$$

The exact solutions of these two equations at $z = h$ can be written as

$$\begin{aligned} \psi(x,h) &= e^{hL_1}\psi(x,0), \\ \psi(x,h) &= e^{hL_2}\psi(x,0), \end{aligned} \tag{3.19}$$

respectively. Suppose the exact solution of Eq. (3.16) is not easily obtained and the solutions of the split equations (3.18) can be obtained easily. In that case, the split-step method aims to converge to the exact solution (3.17) with a sequence of split operators as

$$e^{h(L_1+L_2)} \approx e^{b_n hL_2} e^{a_n hL_1} e^{b_{n-1} hL_2} e^{a_{n-1} hL_1} \dots e^{b_1 hL_2} e^{a_1 hL_1}, \tag{3.20}$$

where a_i and b_i are constant coefficients. The error can be found by expanding both sides of Eq. (3.20) to the power series in h and then taking the difference of these series. The difference of the series obtained for the left and right sides of Eq. (3.20) is $O\left(h^{n+1}\right)$, then the split-step method is n^{th} order accurate in z.

Let's consider a simple case where a_1 and b_1 are equal to 1 and the other coefficients are equal to 0. Then

$$e^{h(L_1+L_2)} \approx e^{hL_2} e^{hL_1}. \tag{3.21}$$

Power series expansion of the left side is

$$\begin{aligned} e^{h(L_1+L_2)} &= 1 + h(L_1+L_2) + \frac{1}{2}h^2(L_1+L_2)^2 + O\left(h^3\right) \\ &= 1 + hL_1 + hL_2 + \frac{1}{2}h^2L_1^2 + \frac{1}{2}h^2L_1L_2 + \frac{1}{2}h^2L_2L_1 + \frac{1}{2}h^2L_2^2 + O\left(h^3\right) \end{aligned} \tag{3.22}$$

and the right side is

$$\begin{aligned} e^{hL_2}e^{hL_1} &= \left(1 + hL_2 + \frac{1}{2}h^2L_2^2 + O\left(h^3\right)\right).\left(1 + hL_1 + \frac{1}{2}h^2L_1^2 + O\left(h^3\right)\right) \\ &= 1 + hL_1 + \frac{1}{2}h^2L_1^2 + hL_2 + h^2L_2L_1 + \frac{1}{2}h^2L_2^2 + O\left(h^3\right) \\ &= 1 + hL_1 + hL_2 + \frac{1}{2}h^2L_1^2 + \frac{1}{2}h^2L_2^2 + h^2L_2L_1 + O\left(h^3\right). \end{aligned} \tag{3.23}$$

Since

$$S_1(h) \equiv e^{hL_2}e^{hL_1} = e^{h(L_1+L_2)} + O\left(h^2\right), \tag{3.24}$$

this scheme is first-order accurate in z.

Now, let $a_1 = \frac{1}{2}$, $a_2 = \frac{1}{2}$, $b_1 = 1$ and other coefficients be 0. In that case

$$e^{h(L_1+L_2)} \approx e^{\frac{1}{2}hL_1} e^{hL_2} e^{\frac{1}{2}hL_1}. \tag{3.25}$$

Power series expansion of the left side is

$$\begin{aligned} &e^{h(L_1+L_2)} \\ &= 1 + h(L_1+L_2) + \frac{1}{2}h^2\left(L_1^2 + L_1L_2 + L_2L_1 + L_2^2\right) \\ &+ \frac{1}{6}h^3\begin{pmatrix} L_1^3 + L_1^2L_2 + L_1L_2L_1 + L_1L_2^2 \\ + L_2L_1^2 + L_2L_1L_2 + L_2^2L_1 + L_2^3 \end{pmatrix} + O\left(h^4\right) \end{aligned} \tag{3.26}$$

and the right side is

$$\begin{aligned} &e^{\frac{1}{2}hL_1}e^{hL_2}e^{\frac{1}{2}hL_1} \\ &= 1 + h(L_1+L_2) + \frac{1}{2}h^2\left(L_1^2 + L_1L_2 + L_2L_1 + L_2^2\right) \\ &+ h^3\begin{pmatrix} \frac{1}{6}L_1^3 + \frac{1}{8}L_1^2L_2 + \frac{1}{4}L_1L_2L_1 + \frac{1}{8}L_2L_1^2 \\ + \frac{1}{4}L_2^2L_1 + \frac{1}{4}L_1L_2^2 + \frac{1}{6}L_2^3 \end{pmatrix} + O\left(h^4\right). \end{aligned} \tag{3.27}$$

Since

$$S_2(h) \equiv e^{\frac{1}{2}hL_1} e^{hL_2} e^{\frac{1}{2}hL_1} = e^{h(L_1+L_2)} + O\left(h^3\right), \tag{3.28}$$

this symmetric splitting scheme, also called *Strang splitting* [66], is second-order accurate in z.

The accuracy of the method can be increased by taking more terms in Eq. (3.20) and choosing coefficients a_i and b_i properly. But, when the number of terms is large, it will be quite complicated to use the series expansion. A higher-order split-step scheme can be obtained by combining several lower-order schemes instead of using the series expansion [68]. For example, the symmetric product of three quadratic schemes can produce a fourth-order split-step scheme. During this process, the Baker–Campbell–Hausdorff formula [69] is utilized. Then, from the scheme obtained with the symmetric product, the coefficients a_i and b_i in Eq. (3.20) can be found. If these coefficients are taken as in Eq. (3.29), a fourth-order scheme is acquired.

$$\begin{aligned} a_1 &= a_4 = \frac{1}{2}c, \\ a_2 &= a_3 = \frac{1}{2}(1-c), \\ b_1 &= b_3 = c, \\ b_2 &= 1-2c, \\ b_4 &= 0, \end{aligned} \tag{3.29}$$

where $c = \frac{1}{2-2^{1/3}}$. In this thesis, while analyzing the stability of solitons, a_i and b_i coefficients are chosen as in Eq. (3.29), and a fourth-order split-step scheme is used.

3.2.2 Split-step method for nonlinear equations

In this section we explain how the split-step method is used in nonlinear equations

$$\psi_z = L(\psi) + N(\psi), \tag{3.30}$$

where one or both of $L(\psi)$ and $N(\psi)$, which are independent of z, may be nonlinear in ψ.

Split-step schemes designed for linear equations in section 3.2.1 can also be used for nonlinear equations [70]. On the grounds of this, consider that the second-order (Strang-splitting) scheme we designed for linear equations will be applied to Eq. (3.30)

with the initial condition $\psi(x,0)$. Thus, Eq. (3.30) is split into sub-equations

$$\psi_z = L(\psi), \tag{3.31a}$$

$$\psi_z = N(\psi). \tag{3.31b}$$

In the first place, Eq. (3.31a) is integrated by half a step $h/2$ to achieve an transitional solution $\psi_1(x,h/2)$. Afterwards, Eq. (3.31b) is integrated by one step h with the initial condition ψ_1 to obtain another transitional solution $\psi_2(x,h)$. Once and for all, Eq. (3.31a) is integrated by half a step $h/2$ again with the initial condition ψ_2, and the final solution $\psi_3(x,h)$ is acquired. As a consequence, $\psi_3(x,h)$ is the numerical result of the second-order splitting scheme. That is to say, $\psi_3(x,h) = S_2(h)\psi(x,0)$.

The order of accuracy of the schemes applied for linner equations does not give a clue about the order of accuracy in nonlinear equations. On the other hand, it was shown in reference [71] that the order of accuracy for the S_1, S_2 and S_4 schemes of the Gross–Pitaevskii equation is the same as for the linear equations. Later on, in reference [6] it is proved that the order of accuracy found for linear equations of schemes up to S_4 is the same for the general nonlinear equation (3.30). The following shows the application of the first-order split-step method to the NLS equation

$$i\psi_z + \frac{\beta}{2}\psi_{xx} + \gamma_1 |\psi|^2 \psi = 0, \quad \psi_0 = \psi(x, z_0). \tag{3.32}$$

Principally, Eq. (3.32) is split into linear and nonlinear parts L and N

$$L: \quad i\psi_z + \frac{\beta}{2}\psi_{xx} = 0, \tag{3.33a}$$

$$N: \quad i\psi_z + \gamma_1 |\psi|^2 \psi = 0. \tag{3.33b}$$

The solution of Eq. (3.33a) is found out in frequency domain. Therefore, this method is also called the split-step Fourier method (SSFM). The Fourier transform of ψ is shown as $\mathscr{F}(\psi)$, the inverse Fourier transform of $\mathscr{F}(\psi)$ is shown as $\mathscr{F}^{-1}(\mathscr{F}(\psi))$ and

$$\begin{aligned} &\mathscr{F}(\psi) = \widehat{\psi}, \\ &\mathscr{F}^{-1}(\mathscr{F}(\psi)) = \mathscr{F}^{-1}(\widehat{\psi}) = \psi, \\ &\mathscr{F}(\psi_{xx}) = -k^2\widehat{\psi}, \end{aligned} \tag{3.34}$$

where k is the Fourier variable. After Fourier transform, Eq. (3.33a) becomes

$$\frac{d}{dz}\widehat{\psi} = -ik^2\frac{\beta}{2}\widehat{\psi}. \tag{3.35}$$

The exact solution of Eq. (3.35) is as follows

$$\widehat{\psi_1}(k,z) = \widehat{\psi}_0 e^{-ik^2\frac{\beta}{2}z}. \tag{3.36}$$

Then,

$$\widehat{\psi_1}(k,z+h) = \widehat{\psi_1}(k,z)e^{-ik^2\frac{\beta}{2}h}. \tag{3.37}$$

Now it's time to solve Eq. (3.33b). This nonlinear part is solved analytically in the spatial domain. The exact solution of Eq. (3.33b) is as shown in Eq. (3.38)

$$\psi(x,z) = \psi_1 e^{i\gamma_1|\psi|^2 z}. \tag{3.38}$$

In that case,

$$\psi(x,z+h) = \psi(x,z)e^{i\gamma_1|\psi(x,z)|^2 h}. \tag{3.39}$$

As a result, first order splitting scheme for NLS equation can be written as

$$S_1(h) = N_h\left\{L_h\psi(z_0)\right\}. \tag{3.40}$$

Furthermore, second-order and fourth-order schemes correspond to

$$S_2(h) = N_{\frac{h}{2}}\left\{L_h\left\{N_{\frac{h}{2}}\psi(z_0)\right\}\right\} \tag{3.41}$$

and

$$S_4(h) = N_{b_4h}\left\{L_{a_4h}\left\{N_{b_3h}\left\{L_{a_3h}\left\{N_{b_2h}\left\{L_{a_2h}\left\{N_{b_1h}\left\{L_{a_1h}\psi(z_0)\right\}\right\}\right\}\right\}\right\}\right\}\right\}, \tag{3.42}$$

respectively, where a_i and b_i coefficients are as in Eq. (3.29) . Since the linear part of the equation is solved by taking the Fourier transform, the spatial accuracy of SSFM is spectral and the accuracy is very high. Split-step methods give very good results, especially in NLS-type equations.

3.3 Fourier Collocation Method

The Fourier collocation method can be used to obtain the entire spectrum of the linear stability operator L. Consider the following NLS equation

$$i\Psi_z + \nabla^2\Psi + F\left(|\Psi|^2,\mathbf{x}\right)\Psi = 0, \tag{3.43}$$

here $F(\cdot,\cdot)$ is a real-valued function. Eq. (3.43) has solutions of the form

$$\Psi(\mathbf{x},z) = \psi(\mathbf{x})e^{i\mu z}, \tag{3.44}$$

where μ is the propagation constant and $\psi(\mathbf{x})$ is a complex-valued function. The linear stability analysis of the general solitary wave function ψ in equation (3.44) is studied by perturbing it with normal modes as follows

$$\Psi(\mathbf{x},z) = \left\{ \psi(\mathbf{x}) + [g(\mathbf{x}) + h(\mathbf{x})]e^{\lambda z} + [g^*(\mathbf{x}) - h^*(\mathbf{x})]\, e^{\lambda^* z} \right\} e^{i\mu z}, \tag{3.45}$$

where $g(\mathbf{x}), h(\mathbf{x}) \ll 1$ are normal modes and λ is the eigenvalue of this normal modes. By substituting Eq. (3.45) in Eq. (3.43) and then linearizing it, the linear stability eigenvalue problem in Eq. (3.46) is obtained.

$$\mathbf{L}\chi = \lambda\chi, \tag{3.46}$$

where

$$\mathbf{L} = i \begin{bmatrix} G_0 & \nabla^2 + G_1 \\ \nabla^2 + G_2 & -G_0 \end{bmatrix}, \quad \chi = \begin{bmatrix} g \\ h \end{bmatrix}, \tag{3.47}$$

additionally, Chapter 4.2.1 explains in detail how to find Eq. (3.47).
In Eq. (3.47):

$$\begin{aligned} G_0 &= \frac{1}{2}\left(\psi^2 - \psi^{*2}\right) F_{|\psi|^2}\left(|\psi|^2, \mathbf{x}\right), \\ G_1 &= -\mu + F\left(|\psi|^2, \mathbf{x}\right) + \left[|\psi|^2 - \frac{1}{2}\left(\psi^2 + \psi^{*2}\right)\right] F_{|\psi|^2}\left(|\psi|^2, \mathbf{x}\right), \\ G_2 &= -\mu + F\left(|\psi|^2, \mathbf{x}\right) + \left[|\psi|^2 + \frac{1}{2}\left(\psi^2 + \psi^{*2}\right)\right] F_{|\psi|^2}\left(|\psi|^2, \mathbf{x}\right). \end{aligned} \tag{3.48}$$

At this stage, some numerical methods can be used to find the eigenvalues (entire spectrum) of the linear stability operator $\mathbf{L}$. We employed the Fourier collocation method in this thesis. While applying this method, the G_0, G_1, G_2 functions and $\chi = [g,h]^T$ eigenfunction are first expanded into the Fourier series in the range $x = [-L/2, L/2]$:

$$G_j = \sum_n c_n^{(j)} e^{inkx}, \quad j = 0,1,2, \tag{3.49}$$

and

$$\begin{aligned} g(x) &= \sum_n a_n e^{inkx}, \\ h(x) &= \sum_n b_n e^{inkx}, \end{aligned} \tag{3.50}$$

where $k = 2\pi/L$.

Subsequently, Eq. (3.49) and Eq. (3.50) are substituted into Eq. (3.46), and a new system of equations is obtained for the coefficients a_j and b_j:

$$\sum_n c_n^{(0)} a_{j-n} - (kj)^2 b_j + \sum_n c_n^{(1)} b_{j-n} = -i\lambda a_j, \tag{3.51a}$$

$$-(kj)^2 a_j + \sum_n c_n^{(2)} a_{j-n} - \sum_n c_n^{(0)} b_{j-n} = -i\lambda b_j, \tag{3.51b}$$

where j is in the interval $(-\infty, +\infty)$. This interval is reduced to the interval $(-N, +N)$ and the following finite dimensional eigenvalue problem is obtained:

$$i \begin{bmatrix} \mathscr{C}_0 & \mathscr{D} + \mathscr{C}_1 \\ \mathscr{D} + \mathscr{C}_2 & -\mathscr{C}_0 \end{bmatrix} \begin{bmatrix} A \\ B \end{bmatrix} = \lambda \begin{bmatrix} A \\ B \end{bmatrix}, \tag{3.52}$$

where

$$\mathscr{D} = (ik)^2 \operatorname{diag}(-N, -N+1, \ldots, N-1, N)^2, \tag{3.53}$$

and the $\mathscr{C}_0$, $\mathscr{C}_1$ and $\mathscr{C}_2$ matrices are as follows:

$$\mathscr{C} = \begin{bmatrix} c_0 & c_{-1} & \cdots & c_{-N} & & & \\ c_1 & c_0 & c_{-1} & \ddots & \ddots & & \\ \vdots & c_1 & c_0 & \ddots & \ddots & \ddots & \\ c_N & \ddots & \ddots & \ddots & \ddots & \ddots & c_{-N} \\ & c_N & \ddots & \ddots & \ddots & \ddots & \vdots \\ & & \ddots & \ddots & \ddots & \ddots & c_{-1} \\ & & & c_N & \cdots & c_1 & c_0 \end{bmatrix} \tag{3.54}$$

here, coefficients c_n takes the values $c_n^{(j)}$ for matrix $\mathscr{C}_j$, and also

$$A = \begin{bmatrix} a_{-N} \\ a_{-N+1} \\ \vdots \\ a_N \end{bmatrix}, \quad B = \begin{bmatrix} b_{-N} \\ b_{-N+1} \\ \vdots \\ b_N \end{bmatrix}. \tag{3.55}$$

To obtain all eigenvalues in the eigenvalue problem (3.52), which has Fourier coefficients, the QR method [72] can be used. In this thesis, the **"eig"** function in the MATLAB program is utilized while finding the eigenvalues.

4. STABILITY ANALYSIS

Finding soliton solutions of the NLS equation is not enough to understand the physical system. As the optical soliton wave propagates, changes in the behavior and structure of the wave are of great importance. That's why linear and nonlinear stability analyses of solitons are prevalent phenomena. In this thesis, the nonlinear stability analysis was performed by examining whether there was any change in the shape, position and amplitude of the soliton as it propagated in the z-direction. The linear stability analysis was done by examining the linear spectrum of the linear stability operator of the soliton.

4.1 Nonlinear Stability

Solitons are considered nonlinearly stable if their shape, amplitude and position do not change as they propagate. An evolution simulation method can be used to examine these properties. In this thesis, the split-step Fourier method (see Ch. 3.2) is employed. The spatial accuracy of SSFM is spectral and the accuracy is very high. Furthermore, the split-step method has some useful features for NLS-type equations. For example, the power $\int |\psi|^2 dx$, which is noteworthy in evolution simulation, is conserved in both NLS equation and split-step methods.

Consider that Eq. (3.2) is split into linear and nonlinear parts:

$$L: \quad iu_z + \frac{\beta}{2} u_{xx} = 0, \tag{4.1a}$$

$$N: \quad iu_z + \gamma_1 |u|^2 u + \gamma_2 |u|^4 u + V_{\mathscr{P}\mathscr{T}}(x)u + (\tau_r + is_1)\, u \frac{\partial}{\partial x}\left(|u|^2\right) + is|u|^2 \frac{\partial}{\partial x} u = 0. \tag{4.1b}$$

Eq. (4.1a) is solved in frequency domain. Therefore, Fourier transform is applied to Eq. (4.1a):

$$\frac{d}{dz}\widehat{u} = -ik^2 \frac{\beta}{2}\widehat{u}. \tag{4.2}$$

The exact solution of Eq. (4.2) is as follows:

$$\widehat{u}(x,z) = \widehat{u}_0 e^{-ik^2 \frac{\beta}{2} z}. \tag{4.3}$$

Thereafter, Eq. (4.1b) is solved in the spatial domain. The exact solution of Eq. (4.1b) is as shown in Eq. (4.4)

$$u(x,z) = u_0 e^{i\left(\gamma_1|u|^2+\gamma_2|u|^4+V_{\mathscr{P}\mathscr{T}}(x)+(\tau_r+is_1)\frac{\partial}{\partial x}\left(|u|^2\right)+is|u|^2\frac{\partial}{\partial x}\right)z}. \tag{4.4}$$

In the above equation, the Fourier and inverse Fourier transformations of the derivative expressions in the exponent are taken, respectively

$$u(x,z) = u_0 e^{i\left(\gamma_1|u|^2+\gamma_2|u|^4+V_{\mathscr{P}\mathscr{T}}(x)+(\tau_r+is_1)\mathscr{F}^{-1}\left\{ik\mathscr{F}\left\{|u|^2\right\}\right\}+is|u|^2\mathscr{F}^{-1}\{ik\}\right)z}. \tag{4.5}$$

Solutions for both linear and nonlinear parts were found. Now one of the splitting schemes described in chapter 3.2 can be applied. In this thesis, the fourth-order split-step scheme is used and the coefficients are taken as in Eq. (3.29).

4.2 Linear Stability

The linear stability analysis was performed by examining the linear spectrum of the linear stability operator of the soliton.

4.2.1 Linear spectrum

The eigenvalues of the soliton's linear stability operator, namely the linear spectrum of the soliton, contain essential information about linear stability. If the real part of any eigenvalues found in the linear spectrum is positive, the soliton is linearly unstable. The larger the positive real parts, the bigger the perturbation growth rate of the soliton. On the other hand, if the eigenvalues in the spectrum are purely imaginary, then some oscillations occur. In this case, the soliton can be considered linearly stable.

Consider (1+1)D CQNLS equation (3.2) as having general type of nonlinearities as follows:

$$iu_z + \frac{\beta}{2}u_{xx} + F\left(|u|^2\right)u + V_{\mathscr{P}\mathscr{T}}(x)u + (\tau_r+is_1)\,u\frac{\partial}{\partial x}\left(|u|^2\right) + is|u|^2\frac{\partial}{\partial x}u = 0, \tag{4.6}$$

where $F(\cdot) \in \mathbb{R}$ and $F(0) = 0$. As shown in Chapter 3, Eq. (4.6) has a soliton solution of the form:

$$u(x,z) = f(x)e^{i\mu z}, \tag{4.7}$$

where $f(x)$ is a complex-valued function and $\lim_{(x,y)\to\pm\infty} f(x) = 0$. Considering the following expressions:

$$\begin{aligned}
&u_z(x,z) = i\mu f e^{i\mu z},\\
&u_x(x,z) = f_x e^{i\mu z},\\
&u_{xx}(x,z) = f_{xx} e^{i\mu z},\\
&|u(x,z)|^2 = uu^* = f e^{i\mu z}\cdot f e^{-i\mu z} = |f|^2,\\
&\left(|u(x,z)|^2\right)_x = 2|f||f|_x,
\end{aligned} \tag{4.8}$$

and substituting in Eq. (4.6), Eq. (4.9) is obtained :

$$\begin{aligned}
&-\mu f e^{i\mu z} + \frac{\beta}{2} f_{xx} e^{i\mu z} + F\left(|f|^2\right) f e^{i\mu z} + V f e^{i\mu z}\\
&+2f\left(\tau_r + i s_1\right)|f||f|_x e^{i\mu z} + i s |f|^2 f_x e^{i\mu z} = 0.
\end{aligned} \tag{4.9}$$

Eq. (4.9) is simplified by discarding the exponential terms:

$$-\mu f + \frac{\beta}{2} f_{xx} + F\left(|f|^2\right) f + V f + 2f\left(\tau_r + i s_1\right)|f||f|_x + i s |f|^2 f_x = 0. \tag{4.10}$$

To analyze the linear stability, equation (4.7) is perturbed as follows:

$$u(x,z) = \left[f(x) + g(x) e^{\lambda z} + h^*(x) e^{\lambda^* z}\right] e^{i\mu z}, \tag{4.11}$$

where g and h are perturbation eigenfunctions and λ is the eigenvalue.

$$\begin{aligned}
u_z &= \left(\lambda g e^{\lambda z} + \lambda^* h^* e^{\lambda^* z} + i\mu f + i\mu g e^{\lambda z} + i\mu h^* e^{\lambda^* z}\right) e^{i\mu z},\\
u_{xx} &= \left(f_{xx} + g_{xx} e^{\lambda z} + h^*_{xx} e^{\lambda^* z}\right) e^{i\mu z}.
\end{aligned} \tag{4.12}$$

$$\begin{aligned}
|u|^2 =& uu^* = \left(f + g e^{\lambda z} + h^* e^{\lambda^* z}\right) e^{i\mu z}\left(f^* + g^* e^{\lambda^* z} + h e^{\lambda z}\right) e^{-i\mu z}\\
=& f f^* + f g^* e^{\lambda^* z} + f h e^{\lambda z} + f^* g e^{\lambda z} + g g^* e^{(\lambda+\lambda^*)z}\\
&+ g h e^{2\lambda z} + f^* h^* e^{\lambda^* z} + g^* h^* e^{2\lambda^* z} + h h^* e^{(\lambda+\lambda^*)z}\\
\simeq& |f|^2 + \left(g^* e^{\lambda^* z} + h e^{\lambda z}\right) f + \left(g e^{\lambda z} + h^* e^{\lambda^* z}\right) f^*.
\end{aligned} \tag{4.13}$$

Using linear Taylor expansion $F(x+h) = F(x) + h\cdot F'(x) + O\left(h^2\right)$,

$$\begin{aligned}
F\left(|u|^2\right) &= F\left(|f|^2 + \left[\left(g^* e^{\lambda^* z} + h e^{\lambda z}\right) f + \left(g e^{\lambda z} + h^* e^{\lambda^* z}\right) f^*\right]\right)\\
&\simeq F\left(|f|^2\right) + \left[\left(g^* e^{\lambda^* z} + h e^{\lambda z}\right) f + \left(g e^{\lambda z} + h^* e^{\lambda^* z}\right) f^*\right] F'\left(|f|^2\right).
\end{aligned} \tag{4.14}$$

Hereby,

$$
\begin{aligned}
&F\left(|u|^2\right)ue^{-i\mu z}\\
=&F\left(|f|^2\right)f+\left[\left(g^*e^{\lambda^* z}+he^{\lambda z}\right)f^2+\left(ge^{\lambda z}+h^*e^{\lambda^* z}\right)|f|^2\right]F'\left(|f|^2\right)\\
&+F\left(|f|^2\right)ge^{\lambda z}\\
&+\left[\left(gg^*e^{(\lambda+\lambda^*)z}+ghe^{2\lambda z}\right)f+\left(g^2e^{2\lambda z}+gh^*e^{(\lambda+\lambda^*)z}\right)f^*\right]F'\left(|f|^2\right)\\
&+F\left(|f|^2\right)h^*e^{\lambda^* z}\\
&+\left[\left(g^*h^*e^{2\lambda^* z}+|h|^2e^{(\lambda+\lambda^*)z}\right)f+\left(gh^*e^{(\lambda+\lambda^*)z}+(h^*)^2e^{2\lambda^* z}\right)f^*\right]F'\left(|f|^2\right)\\
\simeq&F\left(|f|^2\right)\left[f+ge^{\lambda z}+h^*e^{\lambda^* z}\right]\\
&+F'\left(|f|^2\right)\left[\left(f^2h+|f|^2g\right)e^{\lambda z}+\left(f^2g^*+|f|^2h^*\right)e^{\lambda^* z}\right].
\end{aligned}
\tag{4.15}
$$

Substituting Eq. (4.11), (4.12) and (4.15) into Eq. (4.6) gives

$$
\begin{aligned}
&i\left(\lambda ge^{\lambda z}+\lambda^*h^*e^{\lambda^* z}+i\mu f+i\mu ge^{\lambda z}+i\mu h^*e^{\lambda^* z}\right)e^{i\mu z}\\
&+\frac{\beta}{2}\left(f_{xx}+g_{xx}e^{\lambda z}+h^*_{xx}e^{\lambda^* z}\right)e^{i\mu z}\\
&+\left\{\begin{array}{l}F\left(|f|^2\right)\left[f+ge^{\lambda z}+h^*e^{\lambda^* z}\right]\\+F'\left(|f|^2\right)\left[\left(f^2h+|f|^2g\right)e^{\lambda z}+\left(f^2g^*+|f|^2h^*\right)e^{\lambda^* z}\right]\end{array}\right\}e^{i\mu z}\\
&+V\left(f+ge^{\lambda z}+h^*e^{\lambda^* z}\right)e^{i\mu z}\\
&+\left(f+ge^{\lambda z}+h^*e^{\lambda^* z}\right)(\tau_r+is_1)\left\{\begin{array}{l}2|f||f|_x\\+\left(g^*_xe^{\lambda^* z}+h_xe^{\lambda z}\right)f\\+f_x\left(g^*e^{\lambda^* z}+he^{\lambda z}\right)\\+\left(g_xe^{\lambda z}+h^*_xe^{\lambda^* z}\right)f^*\\+f^*_x\left(ge^{\lambda z}+h^*e^{\lambda^* z}\right)\end{array}\right\}e^{i\mu z}\\
&+is\left[|f|^2+\left(g^*e^{\lambda^* z}+he^{\lambda z}\right)f+\left(ge^{\lambda z}+h^*e^{\lambda^* z}\right)f^*\right]\left[f_x+g_xe^{\lambda z}+h^*_xe^{\lambda^* z}\right]e^{i\mu z}=0.
\end{aligned}
\tag{4.16}
$$

Equation (4.16) is multiplied by $e^{-i\mu z}$ and then grouped according to the exponential terms. Thus equation (4.17) is obtained.

For simplicity, let's replace the coefficient $(\tau_r + is_1)$ with p:

$$\begin{aligned}
&\left[-\mu f + \frac{\beta}{2} f_{xx} + F\left(|f|^2\right) f + Vf + 2fp|f||f|_x + is|f|^2 f_x\right] \\
&+ \left\{\begin{array}{l} i\lambda g - \mu g + \frac{\beta}{2} g_{xx} + F\left(|f|^2\right) g + \left(f^2 h + |f|^2 g\right) F'\left(|f|^2\right) \\ + Vg + f^2 p h_x + f_x f p h + f p f^* g_x + f p f_x^* g + 2gp|f||f|_x \\ + is|f|^2 g_x + isfhf_x + isf^* g f_x \end{array}\right\} e^{\lambda z} \\
&+ \left\{\begin{array}{l} i\lambda^* h^* - \mu h^* + \frac{\beta}{2} h_{xx}^* + F\left(|f|^2\right) h^* + \left(f^2 g^* + |f|^2 h^*\right) F'\left(|f|^2\right) \\ + Vh^* + f^2 p g_x^* + f_x f p g^* + f p f^* h_x^* + f p f_x^* h^* + h^* 2p|f||f|_x \\ + is|f|^2 h_x^* + isfg^* f_x + isf^* h^* f_x \end{array}\right\} e^{\lambda^* z} \\
&= 0.
\end{aligned} \tag{4.17}$$

As seen in equation (4.10), the first bracket in equation (4.17) is equal to 0. On the other hand, for equation (4.17) to be satisfied, the factors of the $e^{\lambda z}$ and $e^{\lambda^* z}$ terms must be equal to zero. Hereby first,

$$\begin{aligned}
&i\lambda g - \mu g + \frac{\beta}{2} g_{xx} + F\left(|f|^2\right) g + \left(f^2 h + |f|^2 g\right) F'\left(|f|^2\right) \\
&+ Vg + f^2 p h_x + f_x f p h + f p f^* g_x + f p f_x^* g + 2gp|f||f|_x \\
&+ is|f|^2 g_x + isfhf_x + isf^* g f_x = 0,
\end{aligned} \tag{4.18}$$

which can be rewritten as:

$$\begin{aligned}
&g_x\left(fpf^* + is|f|^2\right) + \frac{\beta}{2} g_{xx} \\
&+ g\left(-\mu + F\left(|f|^2\right) + F'\left(|f|^2\right)|f|^2 + V + fpf_x^* + 2p|f||f|_x + isf^* f_x\right) \\
&+ h_x f^2 p + h\left(F'\left(|f|^2\right) f^2 + f_x f p + isf f_x\right) = -i\lambda g.
\end{aligned} \tag{4.19}$$

Secondly, from equation (4.17),

$$\begin{aligned}
&i\lambda^* h^* - \mu h^* + \frac{\beta}{2} h_{xx}^* + F\left(|f|^2\right) h^* + \left(f^2 g^* + |f|^2 h^*\right) F'\left(|f|^2\right) \\
&+ Vh^* + f^2 p g_x^* + f_x f p g^* + f p f^* h_x^* + f p f_x^* h^* + h^* 2p|f|.|f|_x \\
&+ is|f|^2 h_x^* + isfg^* f_x + isf^* h^* f_x = 0,
\end{aligned} \tag{4.20}$$

which can be rewritten as:

$$\begin{aligned}
&h_x^*\left(fpf^* + is|f|^2\right) + \frac{\beta}{2} h_{xx}^* \\
&+ h^*\left(-\mu + F\left(|f|^2\right) + F'\left(|f|^2\right)|f|^2 + V + fpf_x^* + 2p|f|.|f|_x + isf^* f_x\right) \\
&+ g_x^* f^2 p + g^*\left(F'\left(|f|^2\right) f^2 + f_x f p + isf f_x\right) = -i\lambda^* h^*.
\end{aligned} \tag{4.21}$$

The complex conjugate of equation (4.21) is taken:

$$\begin{aligned}
&h_x\left(f^*p^*f-is|f|^2\right)+\frac{\beta}{2}h_{xx}\\
&+h\left(-\mu+F\left(|f|^2\right)+F'\left(|f|^2\right)|f|^2+V^*+f^*p^*f_x+2p^*|f||f|_x-isff_x^*\right)\\
&+g_x\left(f^2\right)^*p^*+g\left(F'\left(|f|^2\right)\left(f^2\right)^*+f_x^*f^*p^*-isf^*f_x^*\right)=i\lambda h.
\end{aligned} \tag{4.22}$$

Then equation (4.22) is multiplied by -1:

$$\begin{aligned}
&-h_x\left(f^*p^*f-is|f|^2\right)-\frac{\beta}{2}h_{xx}\\
&-h\left(-\mu+F\left(|f|^2\right)+F'\left(|f|^2\right)|f|^2+V^*+f^*p^*f_x+2p^*|f||f|_x-isff_x^*\right)\\
&-g_x\left(f^2\right)^*p^*-g\left(F'\left(|f|^2\right)\left(f^2\right)^*+f_x^*f^*p^*-isf^*f_x^*\right)=-i\lambda h.
\end{aligned} \tag{4.23}$$

Equations (4.19) and (4.23) are written in matrix form and the following equation is obtained:

$$\begin{bmatrix}
\left(fpf^*+is|f|^2\right)\partial_x+\frac{\beta}{2}\partial_{xx} & f^2p\partial x+F'\left(|f|^2\right)f^2\\
-\mu+F\left(|f|^2\right)+F'\left(|f|^2\right)|f|^2 & +fpf_x+isff_x\\
+V+fpf_x^*+2p|f||f|_x+isf^*f_x & \\
 & \\
 & \\
-\left(f^2\right)^*p^*\partial_x-F'\left(|f|^2\right)\left(f^2\right)^* & -\left(f^*p^*f-is|f|^2\right)\partial_x-\frac{\beta}{2}\partial_{xx}\\
-f^*p^*f_x^*+isf^*f_x^* & +\mu-F\left(|f|^2\right)-F'\left(|f|^2\right)|f|^2\\
 & -V^*-f^*p^*f_x-2p^*|f||f|_x+isff_x^*
\end{bmatrix}\begin{bmatrix} g\\ \\ h\end{bmatrix}=-i\lambda\begin{bmatrix} g\\ \\ h\end{bmatrix}. \tag{4.24}$$

Or it can be expressed briefly as follows:

$$i\begin{bmatrix} L_1 & L_2\\ \\ -L_2^* & -L_1^*\end{bmatrix}\begin{bmatrix} g\\ \\ h\end{bmatrix}=\lambda\begin{bmatrix} g\\ \\ h\end{bmatrix}, \tag{4.25}$$

where

$$\begin{aligned}
L_1=&\left(fpf^*+is|f|^2\right)\partial_x+\frac{\beta}{2}\partial_{xx}-\mu+F\left(|f|^2\right)+F'\left(|f|^2\right)|f|^2\\
&+V+fpf_x^*+2p|f||f|_x+isf^*f_x\\
L_2=&f^2p\partial x+F'\left(|f|^2\right)f^2+f_xfp+isff_x.
\end{aligned} \tag{4.26}$$

If Eq. (4.6) has the cubic-quintic nonlinearity:

$$\begin{aligned}
F(x)&=\gamma_1x+\gamma_2x^2,\\
F'(x)&=\gamma_1+2\gamma_2x.
\end{aligned} \tag{4.27}$$

In this case,

$$\begin{aligned} L_1 &= \left(fpf^* + is|f|^2\right)\partial_x + \frac{\beta}{2}\partial_{xx} - \mu + 2\gamma_1|f|^2 + 3\gamma_2|f|^4 \\ &\quad + V + fpf_x^* + 2p|f||f|_x + isf^*f_x \\ L_2 &= f^2p\partial x + \gamma_1 f^2 + 2\gamma_2|f|^2f^2 + f_xfp + isff_x. \end{aligned} \tag{4.28}$$

If Eq. (4.6) has only the cubic nonlinearity, then Eq. (4.28) is written as follows:

$$\begin{aligned} L_1 &= \left(fpf^* + is|f|^2\right)\partial_x + \frac{\beta}{2}\partial_{xx} - \mu + 2\gamma_1|f|^2 \\ &\quad + V + fpf_x^* + 2p|f||f|_x + isf^*f_x \\ L_2 &= f^2p\partial x + \gamma_1 f^2 + f_xfp + isff_x. \end{aligned} \tag{4.29}$$

Eq. (4.25), which is an eigenvalue problem, can be solved numerically to obtain the linear stability spectrum. In this thesis, the Fourier collocation method, described in Chapter 3.3, is used to solve equation (4.25).

5. SOLITONS OF THE NLS EQUATION WITH THE SELF-STEEPENING EFFECT

It is well known that NLS equation (1.1) has stable fundamental soliton solutions (see Figure 2.1). However, higher-order effects might disrupt the stability of the solitons. In this chapter, the dynamic properties of solitons obtained from the NLS equation with the self-steepening term are investigated. In addition, the relationship between $\mathscr{P}\mathscr{T}$-symmetric periodic potential (2.10) and the influences of the self-steepening effect is examined.

5.1 Optical Solitons with the Self-Steepening Effect

We consider the NLS equation with the self-steepening effect as follows

$$iu_z + \frac{\beta}{2}u_{xx} + \gamma_1|u|^2u + is\frac{\partial}{\partial x}\left(|u|^2u\right) = 0. \tag{5.1}$$

Here u is the envelope function which is proportional to the electric field, z is the propagation direction of optical pulse, γ_1 is the coefficient of the cubic nonlinear term, β is the group velocity dispersion (GVD) coefficient, and s is the self-steepening coefficient.

The term GVD dampens the self-steepening effect. This means that as the β coefficient increases, soliton solutions of Eq. (5.1) can be found for larger values of s. In figure 5.1, the solution region of Eq. (5.1) is examined according to the values of s and β. The solutions were tried to be obtained numerically by the pseudospectral renormalization method. While Eq. (5.1) has a soliton solution for the s and β values corresponding to the green dots, no soliton solution can be obtained for the values corresponding to the black dots. As can be seen from the figure, the increase in β while searching for a soliton solution reduces the self-steepening effect.

In Figure 5.2, it is depicted whether a soliton solution of Eq. (5.1) can be found at which values of the s coefficient between 0 and 2 in cases where β has three different values. When the β coefficient is equal to 1, no soliton solution can be found for values

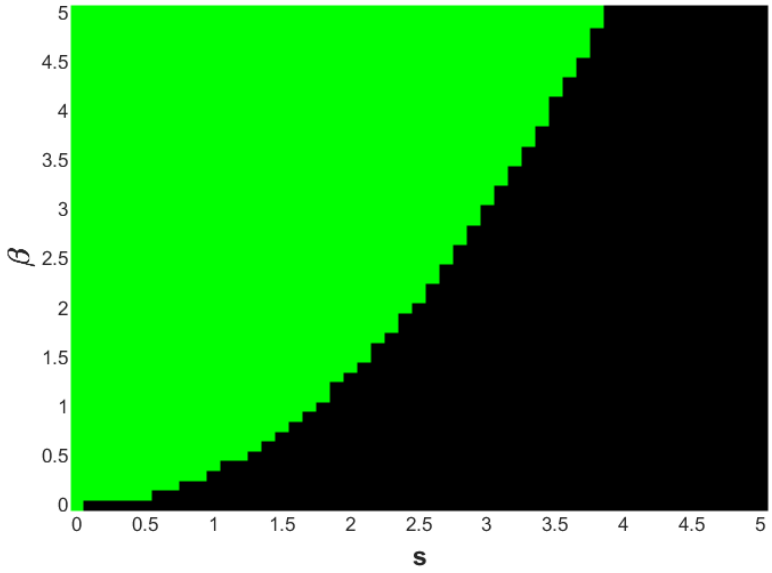

Figure 5.1 : The existence of soliton solutions of Eq. (5.1) with respect to s and β, ($\gamma_1 = 1$).

of s greater than 1.71, whereas when the β coefficient is 1.4, there is a soliton solution for all values of s between 0 and 2.

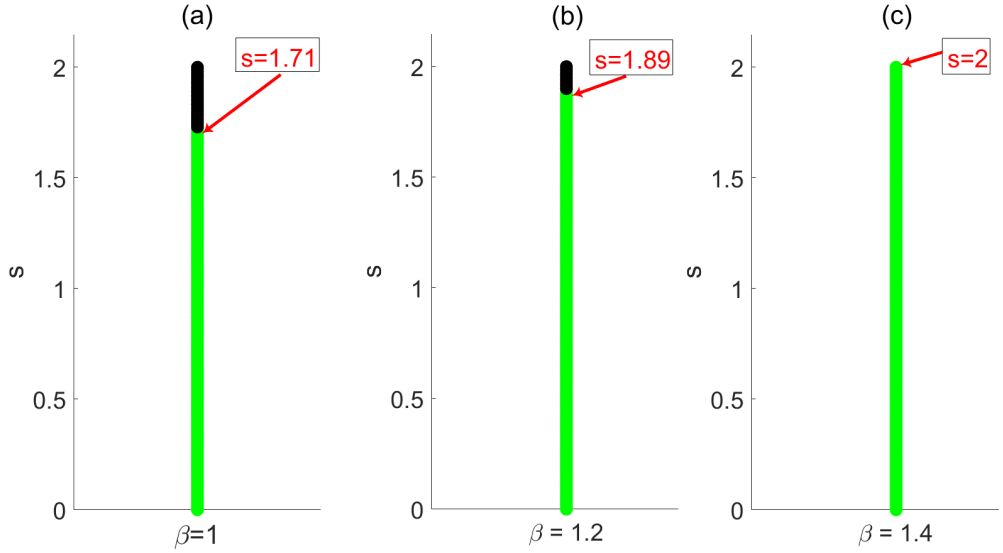

Figure 5.2 : The existence of soliton solutions of Eq. (5.1) with respect to s and β, ($\gamma_1 = 1$).

In Figure 5.3, the value of β is taken as 1 and the soliton solutions obtained from Eq. (5.1) are shown for cases where s is 0, 0.1 and 0.3. As can be seen from the figure, the amplitude of the soliton solutions decreases as the value of s increases.

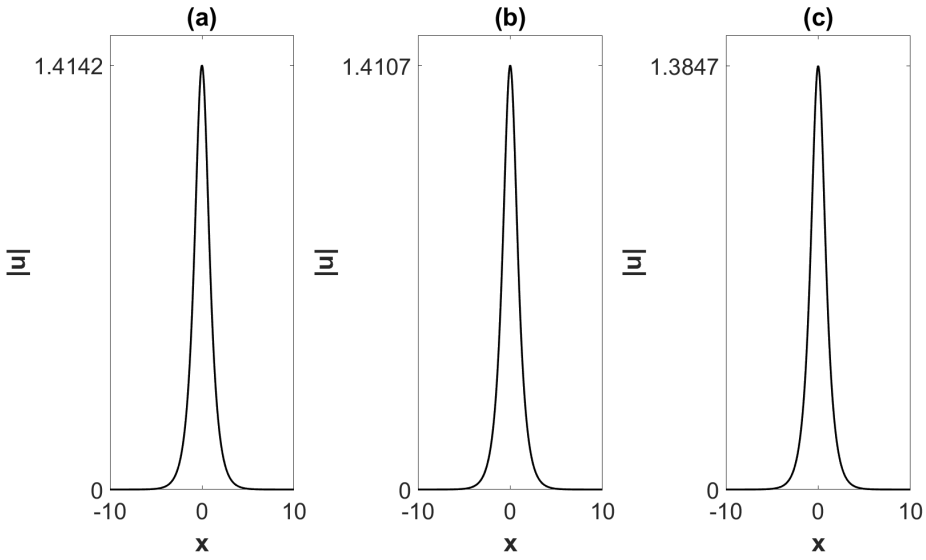

Figure 5.3 : Soliton solutions of Eq. (5.1) ($\beta = 1$, $\gamma_1 = 1$), (a) $s = 0$, (b) $s = 0.1$, (c) $s = 0.3$.

In Figure 5.4, while the value of s is 0.1, the soliton solution obtained from Eq. (5.1) is advanced in the z-direction with the SSFM and its nonlinear stability is examined. At the end of 50 steps, the self-steepening effect shifted the position of the peak of the soliton from $x = 0$ to $x = -4.18$ and increased the amplitude of the soliton from 1.4107 to 1.4839.

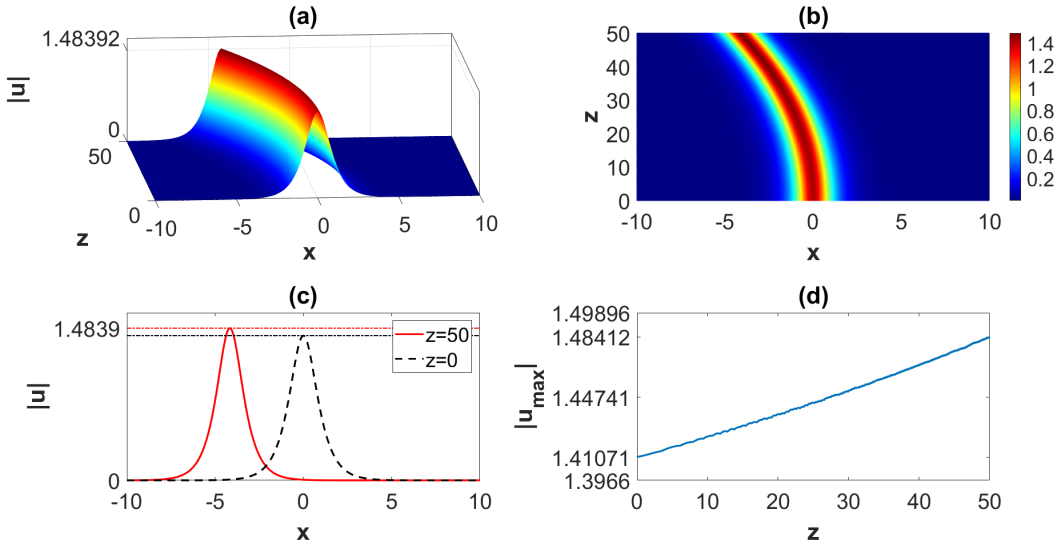

Figure 5.4 : Nonlinear evolution of the soliton solution of Eq. (5.1) ($\beta = 1$, $\gamma_1 = 1$, $s = 0.1$), (a) Three-dimensional view, (b) View from top, (c) Optical pulses at $z = 0$ and $z = 50$, (d) Maximum amplitude as a function of the propagation distance z.

In Figure 5.5, changes in the dynamic properties of the soliton are seen when the s coefficient is increased from 0.1 to 0.3. Although the number of steps is reduced from 50 to 20, the increase in the amplitude of the soliton is considerably higher than when s is 0.1. In addition, in Figure 5.6, the position shifts that occur as the soliton moves towards $z = 20$ are compared in two different cases where the value of the s coefficient is 0.1 and 0.3. It is deduced from Figure 5.6 that as the amplitudes of the solitons increase, the rate of change in their positions also increases.

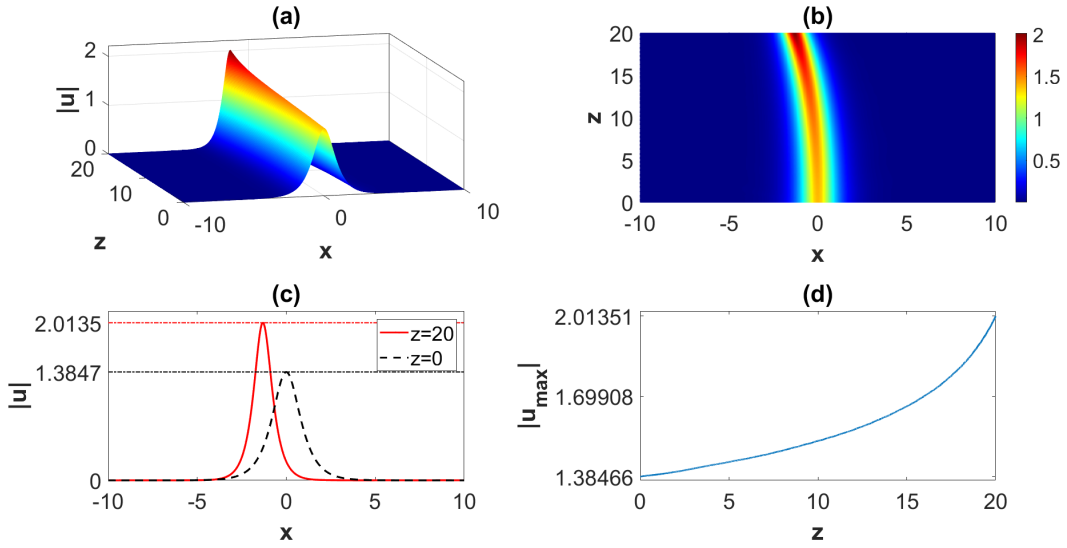

Figure 5.5 : Nonlinear evolution of the soliton solution of Eq. (5.1) ($\beta = 1$, $\gamma_1 = 1$, $s = 0.3$), (a) Three-dimensional view, (b) View from top, (c) Optical pulses at $z = 0$ and $z = 20$, (d) Maximum amplitude as a function of the propagation distance z.

As can be seen from Figure 5.4 and Figure 5.5, the self-steepening effect seriously damages the nonlinear stability of solitons. Although the β coefficient is important for the existence of solitons, it does not have much positive effect on the stability of solitons.

Figure 5.7 shows the linear stability spectrum of solitons obtained from Eq. (5.1) in three different cases where the value of s is 0, 0.1 and 0.3. In all three cases, the real parts of the eigenvalues in the spectrum are equal to zero. This means that the self-steepening effect does not affect the linear stability of the solitons.

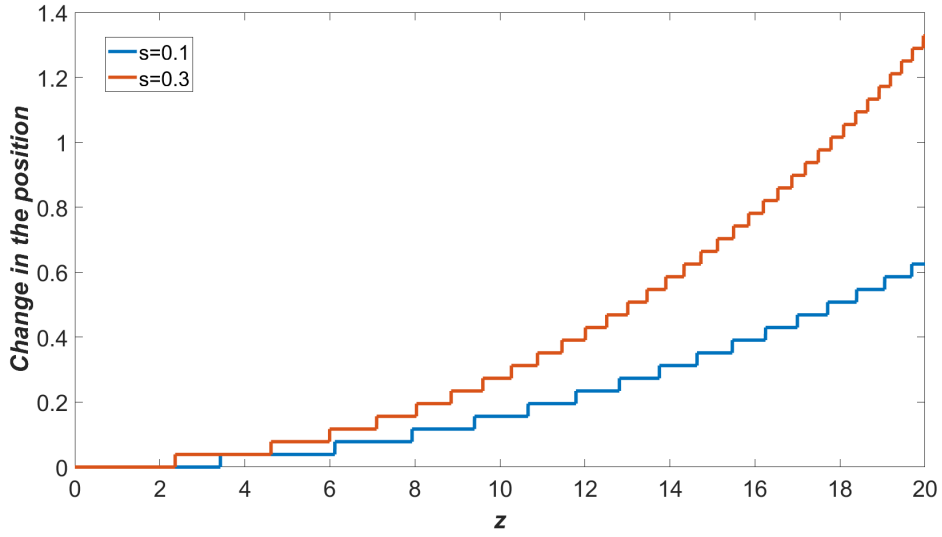

Figure 5.6 : Changes in the position of the vertex of the soliton when s =0.1 and 0.3.

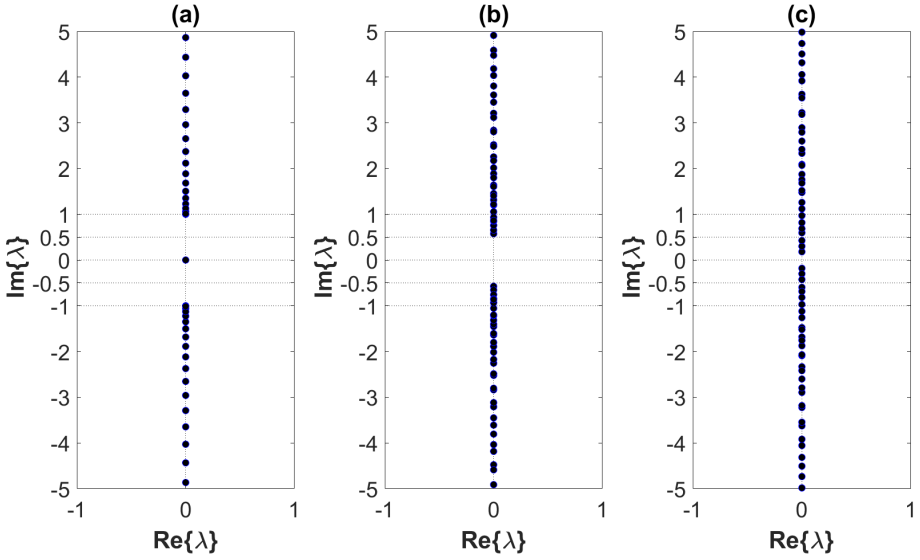

Figure 5.7 : Linear stability spectrum of the soliton solution of Eq. (5.1) when $\beta = 1$ and $\gamma_1 = 1$, (a) $s = 0$, (b) $s = 0.1$, (c) $s = 0.3$.

5.2 Optical Solitons with the Self-Steepening Effect and a Periodic Potential

In this part of the thesis, the instability caused by the self-steepening effect on optical solitons is tried to be eliminated by adding the real part of $\mathscr{PT}$- symmetric periodic potential (2.10) to equation (5.1):

$$iu_z + \frac{\beta}{2}u_{xx} + \gamma_1|u|^2u + V(x) + is\frac{\partial}{\partial x}\left(|u|^2u\right) = 0. \qquad \textbf{(5.2)}$$

Here the periodic potential is as follows

$$V(x) = V_0 \cos^2(x). \tag{5.3}$$

While finding soliton solutions with the PSR method there is an important relationship between the coefficient V_0 and the propagation constant μ, which affects the existence of solitons. This relationship is shown in Figure 5.8 by finding solution regions of Eq. (5.2) according to the V_0 and μ coefficients. In Figure 5.8, Eq. (5.2) has a soliton solution for the V_0 and μ values corresponding to the green dots, while it has no soliton solution for the values corresponding to the black dots. As can be seen in the figure, if the V_0 coefficient increases, μ must increase linearly so that a solution can be found. In this thesis, the propagation constant μ is taken as 1 unless otherwise stated. Therefore, in this chapter, while examining the existence and stability of solitons, the values of the V_0 coefficient between 0 and 1 are taken into account. Because when the coefficient V_0 is slightly greater than 1, the propagation constant μ needs to be increased as well.

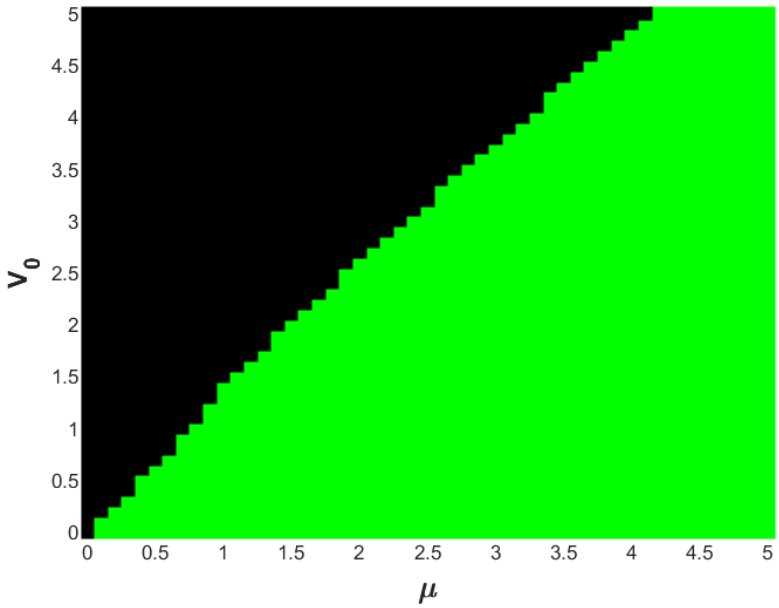

Figure 5.8 : The existence of soliton solutions of Eq. (5.2) with respect to V_0 and μ, ($\gamma_1 = 1, s = 0$).

Figure 5.9 shows whether Eq. (5.2) has a soliton solution or not, according to the values of the s and V_0 coefficients. As can be seen in the figure, as the V_0 coefficient gets larger, a soliton solution can be found for larger s coefficients. Namely, the V_0 coefficient is an important parameter in determining the existence regions of solitons.

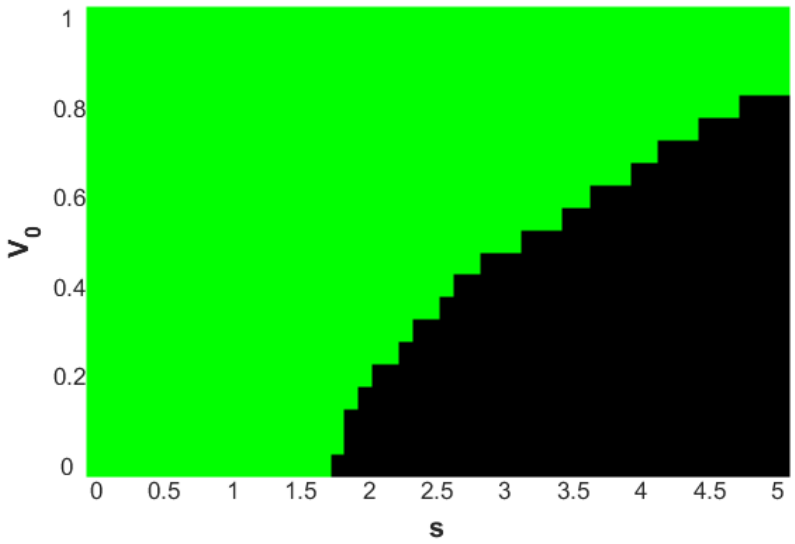

Figure 5.9 : The existence of soliton solutions of Eq. (5.2) with respect to s and V_0, ($\gamma_1 = 1$).

Figure 5.10 shows the effect of V_0 coefficient on nonlinear stability. In Figure 5.10, firstly, the s coefficient is taken as 0.1 in Eq. (5.2) and solitons are found for the values of V_0 between 0 and 1. Then, these solitons are advanced up to $z = 50$ by SSFM, and the differences between the amplitudes and positions of the solitons at $z = 0$ and $z = 50$ are depicted. It is clearly seen that the variation in the amplitudes of the solitons decreases as V_0 increases. In addition, the change in the positions of the solitons has completely disappeared in almost all of the values where V_0 is greater than 0.

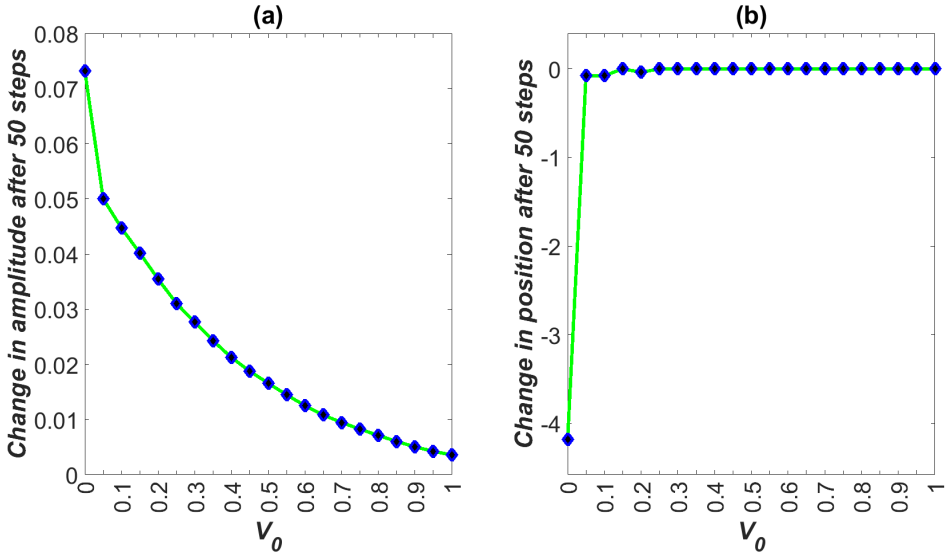

Figure 5.10 : The relationship between the instability caused by the self-steepening and the potential depth V_0 ($s = 0.1$).

Figure 5.11 and Figure 5.12 show the propagation of solitons obtained from Eq. (5.2) for $V_0 = 0.8$ and $V_0 = 1$, respectively. In both cases, it is seen that the potential (5.3) eliminates the position shift. Furthermore, the addition of potential (5.3) reduced the variation in amplitudes from the order of 10^{-2} (see Fig. 5.4) to the order of 10^{-3}.

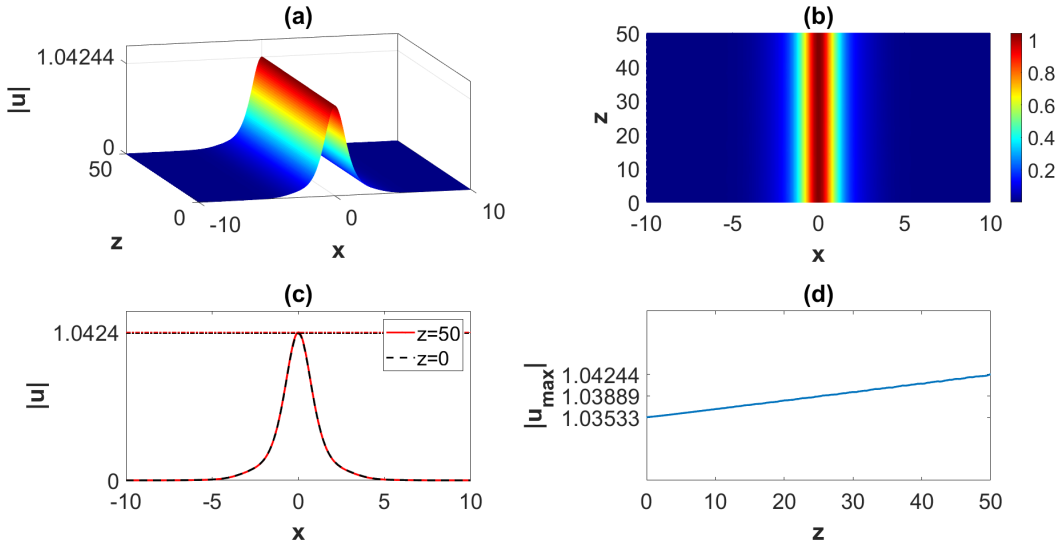

Figure 5.11 : Nonlinear evolution of the soliton solution of Eq. (5.2) ($\beta = 1$, $\gamma_1 = 1$, $s = 0.1$, $V_0 = 0.8$), (a) Three-dimensional view, (b) View from top, (c) Optical pulses at $z = 0$ and $z = 50$, (d) Maximum amplitude as a function of the propagation distance z.

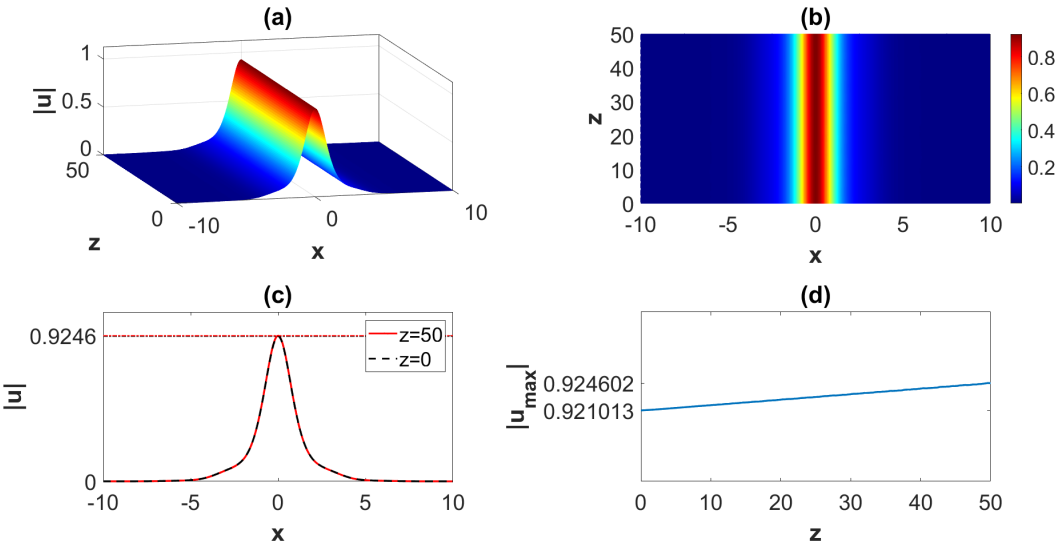

Figure 5.12 : Nonlinear evolution of the soliton solution of Eq. (5.2) ($\beta = 1$, $\gamma_1 = 1$, $s = 0.1$, $V_0 = 1$), (a) Three-dimensional view, (b) View from top, (c) Optical pulses at $z = 0$ and $z = 50$, (d) Maximum amplitude as a function of the propagation distance z.

Figure 5.13 shows the linear stability spectrum of solitons obtained from Eq. (5.2) in three different cases where the value of V_0 is 0.5, 0.8 and 1. In all three cases, the real

parts of the eigenvalues in the spectrum are equal to zero. This means that potential (5.3) does not damage the linear stability of the solitons.

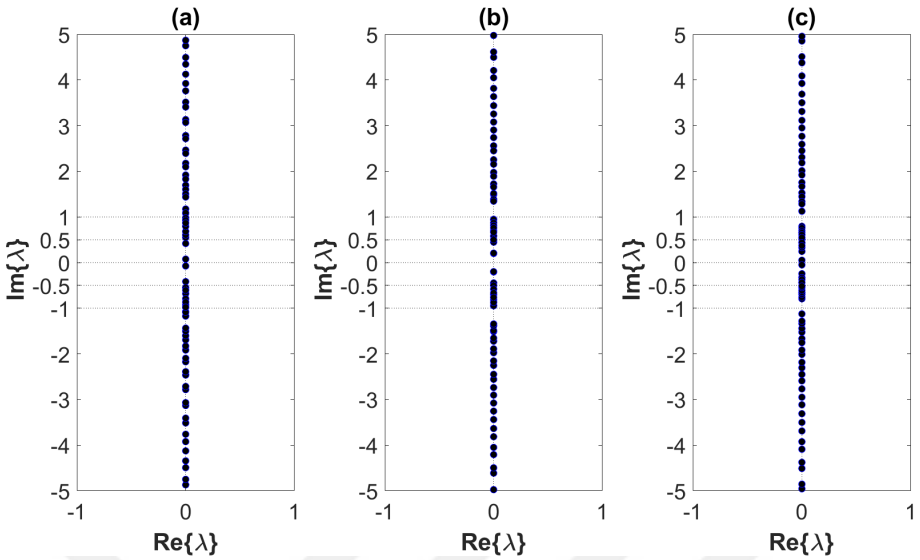

Figure 5.13 : Linear stability spectrum of the soliton solution of Eq. (5.2) ($\beta = 1$, $\gamma_1 = 1$, $s = 0.1$), (a) $V_0 = 0.5$, (b) $V_0 = 0.8$, (c) $V_0 = 1$.

5.3 Optical Solitons with the Self-Steepening Effect and a $\mathscr{PT}$- Symmetric Periodic Potential

In the previous section, the instability of solitons was largely eliminated by adding potential (5.3) to the NLS equation with the self-steepening term. The position shift observed in solitons was completely fixed and the variation in amplitude was reduced to the order of 10^{-3}. In this section, the variation in the amplitudes of the solitons during propagation is tried to be reduced further by adding the $\mathscr{PT}$- symmetric periodic potential (2.10) to Eq. (5.1):

$$iu_z + \frac{\beta}{2}u_{xx} + \gamma_1|u|^2u + V_{\mathscr{PT}}(x) + is\frac{\partial}{\partial x}\left(|u|^2u\right) = 0. \tag{5.4}$$

Figure 5.14 shows the propagation of the soliton obtained from Eq. (5.4) when $s = 0.1$, $V_0 = 0.7$ (depth of the real part of the potential), $W_0 = 0.29135$ (depth of the imaginary part of the potential). It is clearly seen from Figure 5.14 that stable solitons can be obtained with the use of the $\mathscr{PT}$- symmetric periodic potential. $\mathscr{PT}$- symmetric periodic potential (2.10) has completely eliminated the position shift phenomenon caused by the self-steepening effect. It also reduced the difference between the amplitudes of the obtained soliton at z=50 and z=0 to the order of 10^{-7}.

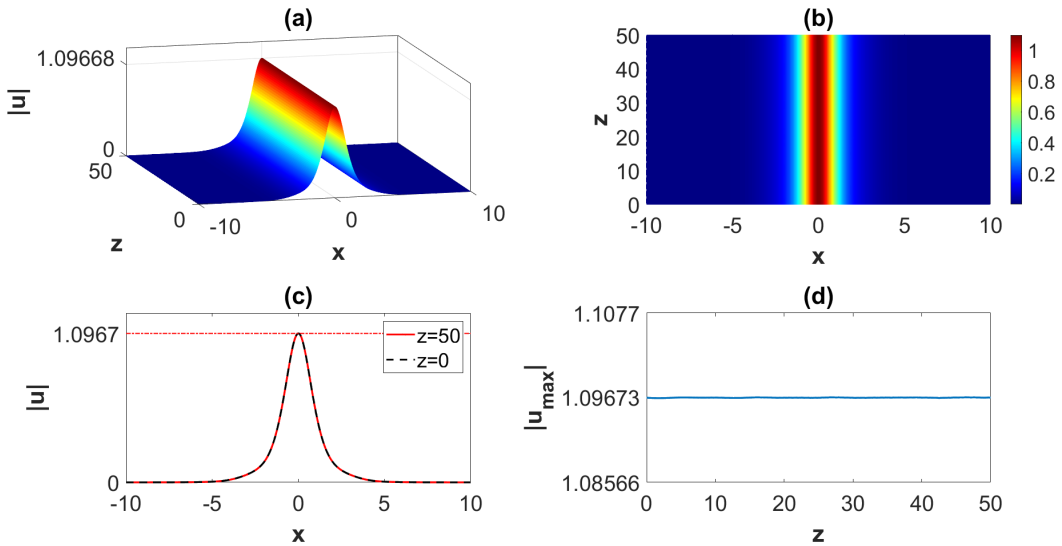

Figure 5.14 : Nonlinear evolution of the soliton solution of Eq. (5.4) ($\beta = 1$, $\gamma_1 = 1$, $s = 0.1$, $V_0 = 0.7$, $W_0 = 0.29135$), (a) Three-dimensional view, (b) View from top, (c) Optical pulses at $z = 0$ and $z = 50$, (d) Maximum amplitude as a function of the propagation distance z.

Figure 5.15 shows the effect of the imaginary part of the potential on the linear stability spectrum of solitons. In Figure 5.15 (a) and 5.15 (b), the V_0 coefficient is 0, while the W_0 coefficient is 0.1 and 0.2, respectively. In both cases, since the real part of some eigenvalues in the spectrum is different from zero, it can be said that the imaginary part of the potential negatively affects the linear stability of the solitons. In Figure 5.15 (c), W_0 was taken as 0.2 again and the value of the V_0 coefficient was increased to 1. In this case, the V_0 coefficient eliminated the negative effect of the W_0 coefficient and the soliton became linearly stable.

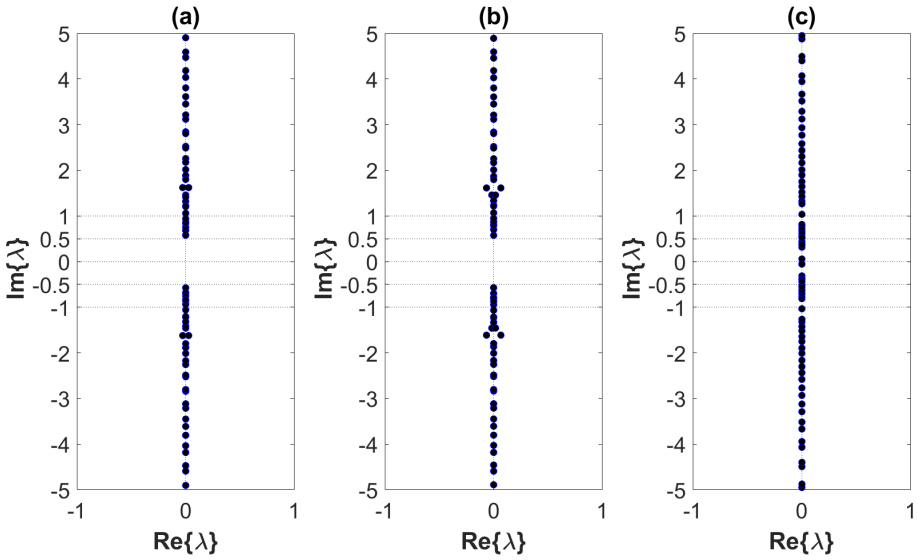

Figure 5.15 : Linear stability spectrum of the soliton solution of Eq. (5.4) ($\beta = 1$, $\gamma_1 = 1$, $s = 0.1$), (a) $V_0 = 0, W_0 = 0.1$, (b) $V_0 = 0, W_0 = 0.2$, (c) $V_0 = 1, W_0 = 0.2$.

6. SOLITONS OF THE CQNLS EQUATION WITH THE SELF-STEEPENING EFFECT

In this chapter, soliton solutions of the CQNLS equation with the self-steepening term are examined. This equation can be written as

$$iu_z + \frac{\beta}{2}u_{xx} + \gamma_1 |u|^2 u + \gamma_2 |u|^4 u + is\frac{\partial}{\partial x}\left(|u|^2 u\right) = 0, \qquad \textbf{(6.1)}$$

where u is the envelope function which is proportional to the electric field, z is the propagation direction of optical pulse, β is the group velocity dispersion (GVD) coefficient, s is the self-steepening coefficient and, γ_1 and γ_2 are the coefficients of the cubic and quintic nonlinear terms, respectively. Different types of media can be defined according to whether γ_1 and γ_2 are positive or negative. The positive sign indicates the nonlinear optical process is self-focusing and the negative sign indicates the nonlinear optical process is self-defocusing. In this chapter, we will only work on a self-focusing cubic, self-defocusing quintic medium ($\gamma_1 = 1$, $\gamma_2 = -1$).

In Figure 6.1 , the existence of soliton solutions of Eq. (6.1) according to the values of the s and β coefficients are examined. In the figure, the green areas represent the regions where soliton solutions are found, the black areas represent the regions where soliton solutions can not be found. When Figure 6.1 is compared with Figure 5.1, it is seen that Eq. (6.1) has a much larger solution area than Eq. (5.1).

In Figure 6.2, the value of β is taken as 1 and the soliton solutions obtained from Eq. (6.1) are shown for cases where s is 0, 0.1 and 0.3. It can be seen from the figure that the amplitude of the solitons decreases as the self-steepening effect increases.

In Figure 6.3, while the value of s is 0.1, the soliton solution obtained from Eq. (6.1) is advanced in the z-direction with the SSFM and its nonlinear stability is examined. At the end of 50 steps, it is clearly seen that there is no shift in the position of the soliton. In addition, only an increase of the order of 10^{-6} in amplitude was observed.

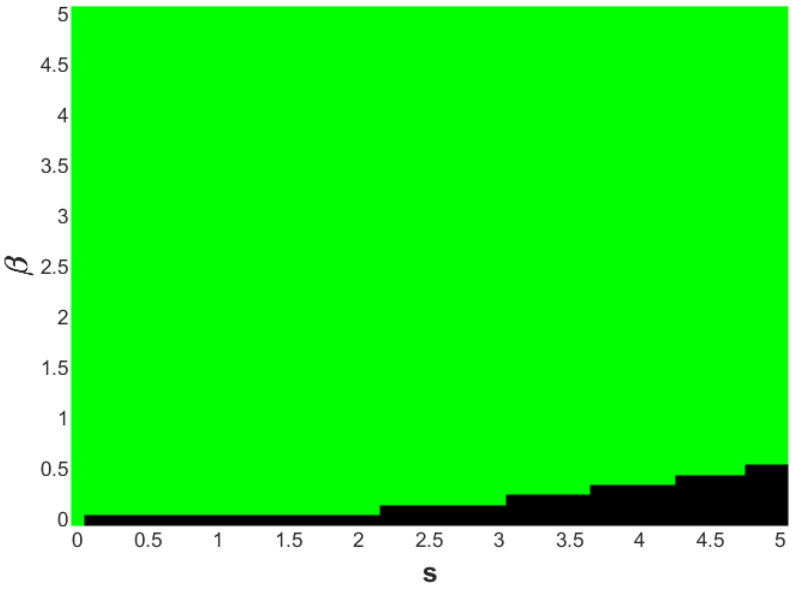

Figure 6.1 : Solution region of Eq. (6.1) with respect to s and β ($\beta = 1$, $\gamma_1 = 1$, $\gamma_2 = -1$).

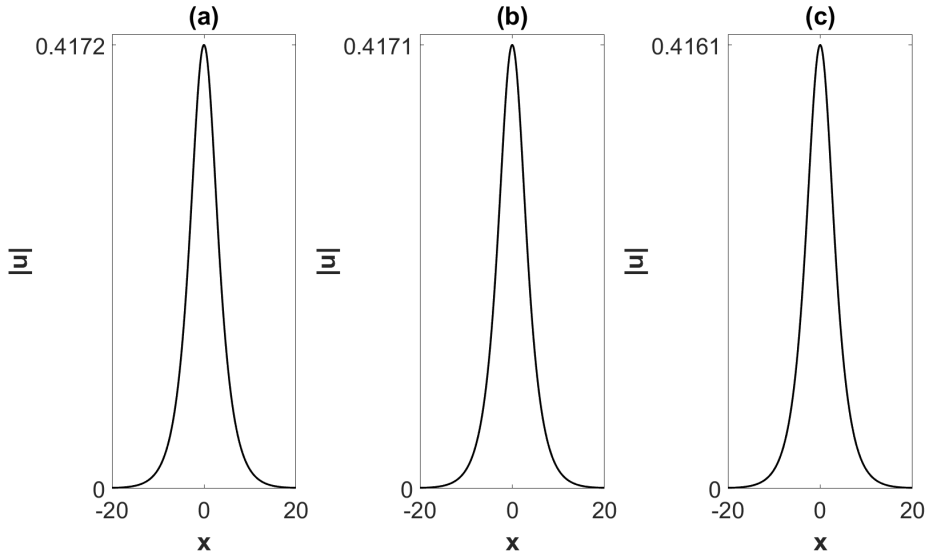

Figure 6.2 : Soliton solutions of Eq. (6.1) ($\beta = 1$, $\gamma_1 = 1$, $\gamma_2 = -1$), (a) $s = 0$, (b) $s = 0.1$, (c) $s = 0.3$.

In Figure 6.4, the s coefficient in Eq. (6.1) is increased from 0.1 to 0.3, and the nonlinear stability of the obtained soliton is investigated. Despite a significant increase in the s coefficient, the soliton continues to maintain its stable structure.

Figure 6.5 shows the linear stability spectrum of solitons obtained from Eq. (6.1) in three different cases where the value of s is 0, 0.1 and 0.3. In all three cases, the real

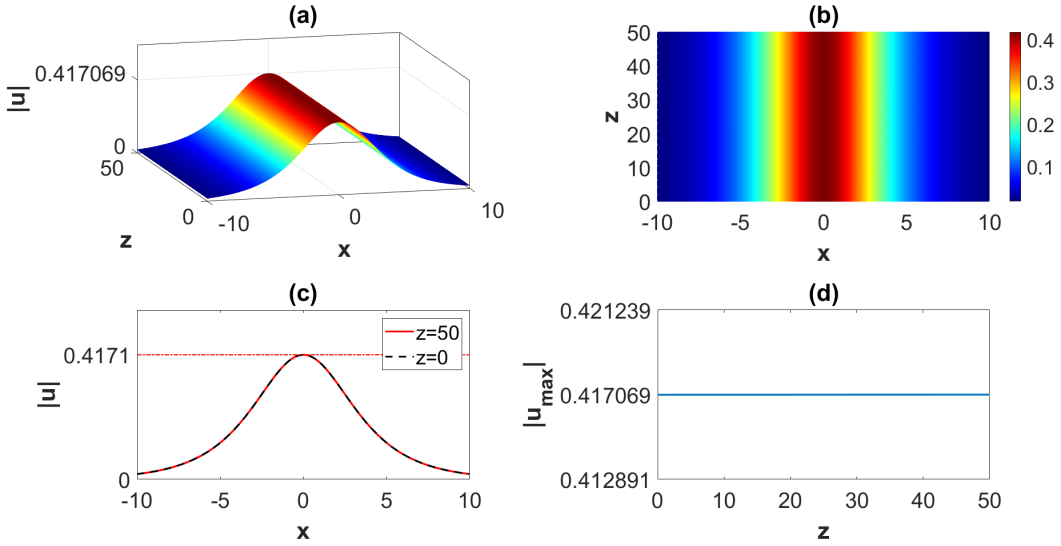

Figure 6.3 : Nonlinear evolution of the soliton solution of Eq. (6.1) ($\beta = 1$, $\gamma_1 = 1$, $\gamma_2 = -1$ $s = 0.1$), (a) Three-dimensional view, (b) View from top, (c) Optical pulses at $z = 0$ and $z = 50$, (d) Maximum amplitude as a function of the propagation distance z.

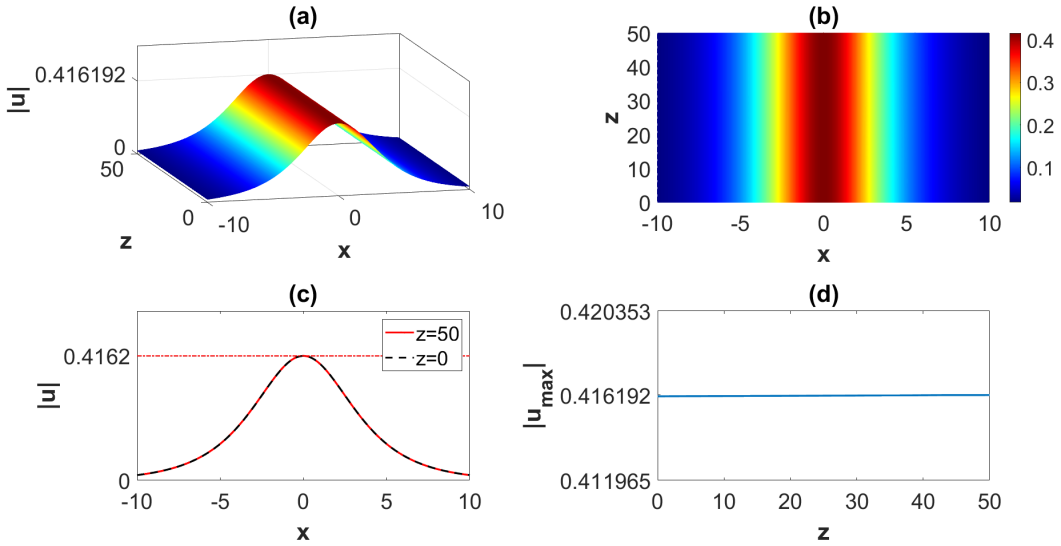

Figure 6.4 : Nonlinear evolution of the soliton solution of Eq. (6.1) ($\beta = 1$, $\gamma_1 = 1$, $\gamma_2 = -1$ $s = 0.3$), (a) Three-dimensional view, (b) View from top, (c) Optical pulses at $z = 0$ and $z = 50$, (d) Maximum amplitude as a function of the propagation distance z.

parts of the eigenvalues in the spectrum are equal to zero. This means that the soliton solutions obtained from Eq. (6.1) are linearly stable under the self-steepening effect.

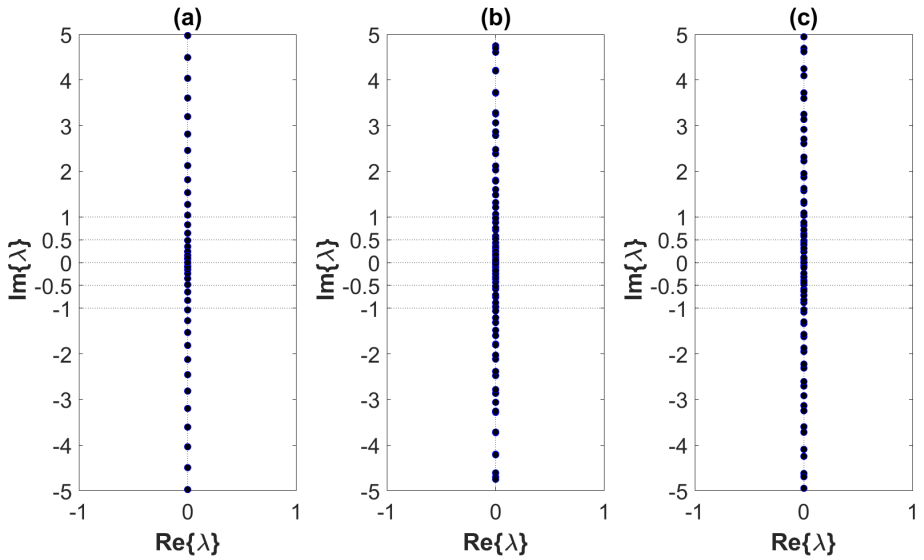

Figure 6.5 : Linear stability spectrum of the soliton solution of Eq. (6.1) ($\beta = 1$, $\gamma_1 = 1$, $\gamma_2 = -1$), (a) $s = 0$, (b) $s = 0.1$, (c) $s = 0.3$.

7. CONCLUSIONS AND RECOMMENDATIONS

In this thesis, the existence and stability of soliton solutions of the NLS and CQNLS equations with the self-steepening effect and $\mathscr{PT}$- symmetric potential were investigated numerically. The pseudospectral renormalization method was used to obtain fundamental soliton solutions. In order to test the nonlinear stability of solitons, spatial evolution simulation of solitons was examined. For this, the split-step Fourier method, which has a very high performance in NLS-type equations, was used. In addition, while examining the dynamic properties of solitons, linear stability conditions were also taken into account. Linear stability analysis of solitons was performed by examining the whole linear stability spectrum of solitons with the help of the Fourier collocation method. The first 4 chapters of this thesis give information about NLS equations, optical solitons, higher-order effects, numerical methods, and stability analysis.

In Chapter 5, the NLS equation with the self-steepening term was analyzed. It was observed that in the absence of the term GVD, the self-steepening effect caused a shock effect on the solitons. It has been shown that the GVD term absorbs the shock effect and the solution sets of solitons expand as the GVD coefficient increases. Although the GVD shows significant resistance to the self-steepening effect, the self-steepening effect severely disrupts the structure of the solitons as they propagate. The self-steepening effect causes solitons to increase in amplitude and shift their position. These negative phenomena were tried to be eliminated with $\mathscr{PT}$- symmetric periodic potential (2.10). It was observed that the real part of the $\mathscr{PT}$- symmetric potential completely eliminates the position shift and also significantly reduces the variation in amplitude. On the other hand, the imaginary part of the potential contributes greatly to the stability of the soliton by further reducing the change in amplitude. The self steepening effect and the $\mathscr{PT}$- symmetric potential have no negative effects on the linear stability of solitons. However, when the imaginary part

of the potential is used alone, the real part of some of the eigenvalues in the spectrum of solitons is different from zero.

Finally, the soliton solutions of the CQNLS equation with the self-steepening term were examined in the self-focusing cubic, self-defocusing quintic medium. It has been shown that the solution set of the CQNLS equation is quite large compared to the solution set of the classical NLS equation. In addition, it has been determined that the solitons obtained here are stable both linearly and nonlinearly.

The studies in this thesis can be extended to different media by change of the signs of the nonlinear coefficients. In addition, the relationship of the self-steepening effect with other higher-order effects can be investigated in future studies.

REFERENCES

[1] **Davydov, A.** (1973). The theory of contraction of proteins under their excitation, *Journal of Theoretical Biology*, *38*(3), 559–569.

[2] **Su, W.P.**, **Schrieffer, J.R. and Heeger, A.J.** (1979). Solitons in Polyacetylene, *Physical Review Letters*, *42*(25), 1698–1701.

[3] **Trombettoni, A. and Smerzi, A.** (2001). Discrete Solitons and Breathers with Dilute Bose-Einstein Condensates, *Physical Review Letters*, *86*(11), 2353–2356.

[4] **Christodoulides, D.N. and Joseph, R.I.** (1988). Discrete self-focusing in nonlinear arrays of coupled waveguides, *Opt. Lett.*, *13*(9), 794–796.

[5] **Hasegawa, A. and Tappert, F.** (1973). Transmission of stationary nonlinear optical pulses in dispersive dielectric fibers. I. Anomalous dispersion, *Applied Physics Letters*, *23*(3), 142–144.

[6] **Yang, J.** (2010). *Nonlinear Waves in Integrable and Non-Integrable Systems*, Society for Industrial and Applied Mathematics, USA.

[7] **Nair, A.A.**, **Porsezian, K. and Jayaraju, M.** (2018). Impact of higher order dispersion and nonlinearities on modulational instability in a dual-core optical fiber, *The European Physical Journal D*, *72*(1).

[8] **Göksel, İ.**, **Antar, N. and Bakırtaş, İ.** (2015). Solitons of $(1+1)$ D cubic-quintic nonlinear Schrödinger equation with $\mathscr{P}\mathscr{T}-$ symmetric potentials, *Optics Communications*, *354*, 277–285.

[9] **Boudebs, G.**, **Cherukulappurath, S.**, **Leblond, H.**, **Troles, J.**, **Smektala, F. and Sanchez, F.** (2003). Experimental and theoretical study of higher-order nonlinearities in chalcogenide glasses, *Optics Communications*, *219*(1-6), 427–433.

[10] **Hasegawa, A. and Kodama, Y.** (1995). *Solitons in Optical Communications*, Oxford series in optical and imaging sciences, Clarendon Press.

[11] **Agrawal, G.P.**, (2019). Chapter 5 - Optical solitons, **G.P. Agrawal**, editor, Nonlinear Fiber Optics (Sixth Edition), Academic Press, sixth edition edition, pp.127–187.

[12] **Thuy, D.T.**, **Vinh, N.T.**, **Thuan, B.D. and Van, C.L.** (2016). Influence of Self-steepening and Higher Dispersion Effects on the Propagation Characteristics of Solitons in Optical Fibers, *computational methods in science and technology*, *22*, 239–243.

[13] **Boardman, A.D. and Cooper, G.S.** (1984). Nonlinear wave propagation in optical fibres, *Applied Scientific Research*, *41*(3-4), 333–343.

[14] **Ohkuma, K.**, **Ichikawa, Y.H. and Abe, Y.** (1987). Soliton propagation along optical fibers, *Opt. Lett.*, *12*(7), 516–518.

[15] **Hodel, W. and Weber, H.P.** (1987). Decay of femtosecond higher-order solitons in an optical fiber induced by Raman self-pumping, *Opt. Lett.*, *12*(11), 924–926.

[16] **Ablowitz, M.J. and Musslimani, Z.H.** (2005). Spectral renormalization method for computing self-localized solutions to nonlinear systems, *Optics Letters*, *30*(16), 2140.

[17] **Russell, J.S.** (1844). Report on waves, *Report of the Fourteenth Meeting of the British Association for the Advancement of Science*, 311–390.

[18] **Korteweg, D.J. and De Vries, G.** (1895). On the change of form of long waves advancing in a rectangular canal, and on a new type of long stationary waves, *The London, Edinburgh, and Dublin Philosophical Magazine and Journal of Science*, *39*(240), 422–443.

[19] **Zabusky, N.J. and Kruskal, M.D.** (1965). Interaction of "Solitons" in a Collisionless Plasma and the Recurrence of Initial States, *Physical Review Letters*, *15*(6), 240–243.

[20] **Benney, D. and Newell, A.** (1967). The propagation of nonlinear wave envelopes, *Journal of mathematics and Physics*, *46*(1-4), 133–139.

[21] **Zakharov, V.E.** (1972). Stability of periodic waves of finite amplitude on the surface of a deep fluid, *Journal of Applied Mechanics and Technical Physics*, *9*(2), 190–194.

[22] **Demartini, F.**, **Townes, C.H.**, **Gustafson, T.K. and Kelley, P.L.** (1967). Self-Steepening of Light Pulses, *Physical Review*, *164*(2), 312–323.

[23] **Kaup, D.J. and Newell, A.C.** (1978). An exact solution for a derivative nonlinear Schrödinger equation, *Journal of Mathematical Physics*, *19*(4), 798–801.

[24] **Nakamura, A. and Chen, H.H.** (1980). Multi-soliton solutions of a derivative nonlinear Schrödinger equation, *Journal of the Physical Society of Japan*, *49*(2), 813–816.

[25] **Steudel, H.** (2003). The hierarchy of multi-soliton solutions of the derivative nonlinear Schrödinger equation, *Journal of Physics A: Mathematical and General*, *36*(7), 1931.

[26] **Moses, J.**, **Malomed, B.A. and Wise, F.W.** (2007). Self-steepening of ultrashort optical pulses without self-phase-modulation, *Physical Review A*, *76*(2), 021802.

[27] **Anderson, D. and Lisak, M.** (1983). Nonlinear asymmetric self-phase modulation and self-steepening of pulses in long optical waveguides, *Physical Review A*, *27*(3), 1393.

[28] **Daoui, A.K.**, **Azzouzi, F.**, **Triki, H.**, **Biswas, A.**, **Zhou, Q.**, **Moshokoa, S.P. and Belic, M.** (2019). Propagation of chirped gray optical dips in nonlinear metamaterials, *Optics Communications*, *430*, 461–466.

[29] **Petviashvili, V.I.** (1976). Equation of an extraordinary soliton, *Fizika Plazmy*, *2*, 469–472.

[30] **Ablowitz, M.J. and Biondini, G.** (1998). Multiscale pulse dynamics in communication systems with strong dispersion management, *Opt. Lett.*, *23*(21), 1668–1670.

[31] **Ablowitz, M.J. and Musslimani, Z.H.** (2001). Discrete Diffraction Managed Spatial Solitons, *Physical Review Letters*, *87*(25).

[32] **Ablowitz, M.J. and Musslimani, Z.H.** (2003). Dark and gray strong dispersion-managed solitons, *Physical Review E*, *67*(2).

[33] **Ablowitz, M.J. and Musslimani, Z.H.** (2003). Discrete spatial solitons in a diffraction-managed nonlinear waveguide array: a unified approach, *Physica D: Nonlinear Phenomena*, *184*(1), 276–303.

[34] **Musslimani, Z.H. and Yang, J.** (2004). Self-trapping of light in a two-dimensional photonic lattice, *J. Opt. Soc. Am. B*, *21*(5), 973–981.

[35] **Lakoba, T. and Yang, J.** (2007). A generalized Petviashvili iteration method for scalar and vector Hamiltonian equations with arbitrary form of nonlinearity, *Journal of Computational Physics*, *226*(2), 1668–1692.

[36] **Antar, N.** (2014). Pseudospectral Renormalization Method for Solitons in Quasicrystal Lattice with the Cubic-Quintic Nonlinearity, *Journal of Applied Mathematics*, *2014*, 1–17.

[37] **Gatz, S. and Herrmann, J.** (1991). Soliton propagation in materials with saturable nonlinearity, *J. Opt. Soc. Am. B*, *8*(11), 2296–2302.

[38] **Hilligsøe, K.M.**, **Paulsen, H.N.**, **Thøgersen, J.**, **Keiding, S.R. and Larsen, J.J.** (2003). Initial steps of supercontinuum generation in photonic crystal fibers, *J. Opt. Soc. Am. B*, *20*(9), 1887–1893.

[39] **Bender, C.M. and Boettcher, S.** (1998). Real Spectra in Non-Hermitian Hamiltonians Having $\mathscr{P}\mathscr{T}-$Symmetry, *Physical 4 Review Letters*, *80*(24), 5243–5246.

[40] **Dietz, B.**, **Harney, H.L.**, **Kirillov, O.**, **Miski-Oglu, M.**, **Richter, A. and Schäfer, F.** (2011). Exceptional points in a microwave billiard with time-reversal invariance violation, *Physical review letters*, *106*(15), 150403.

[41] **Schindler, J.**, **Li, A.**, **Zheng, M.C.**, **Ellis, F.M. and Kottos, T.** (2011). Experimental study of active LRC circuits with PT symmetries, *Physical Review A*, *84*(4), 040101.

[42] **Chong, Y.**, **Ge, L. and Stone, A.D.** (2011). PT-symmetry breaking and laser-absorber modes in optical scattering systems, *Physical Review Letters*, *106*(9), 093902.

[43] **Schomerus, H.** (2010). Quantum noise and self-sustained radiation of PT-symmetric systems, *Physical review letters*, *104*(23), 233601.

[44] **Rüter, C.E.**, **Makris, K.G.**, **El-Ganainy, R.**, **Christodoulides, D.N.**, **Segev, M. and Kip, D.** (2010). Observation of parity–time symmetry in optics, *Nature Physics*, *6*(3), 192–195.

[45] **Regensburger, A.**, **Bersch, C.**, **Miri, M.A.**, **Onishchukov, G.**, **Christodoulides, D.N. and Peschel, U.** (2012). Parity–time synthetic photonic lattices, *Nature*, *488*(7410), 167–171.

[46] **Musslimani, Z.H.**, **Makris, K.G.**, **El-Ganainy, R. and Christodoulides, D.N.** (2008). Optical Solitons in PT Periodic Potentials, *Physical Review Letters*, *100*(3).

[47] **Makris, K.G.**, **El-Ganainy, R.**, **Christodoulides, D.N. and Musslimani, Z.H.** (2011). $\mathscr{P}\mathscr{T}$ -Symmetric Periodic Optical Potentials, *International Journal of Theoretical Physics*, *50*(4), 1019–1041.

[48] **Zeng, J. and Lan, Y.** (2012). Two-dimensional solitons in PT linear lattice potentials, *Physical Review E*, *85*(4).

[49] **Burlak, G. and Malomed, B.A.** (2013). Stability boundary and collisions of two-dimensional solitons in PT-symmetric couplers with the cubic-quintic nonlinearity, *Physical Review E*, *88*(6).

[50] **Ge, L.**, **Shen, M.**, **Zang, T.**, **Ma, C. and Dai, L.** (2015). Stability of optical solitons in parity-time-symmetric optical lattices with competing cubic and quintic nonlinearities, *Physical Review E*, *91*(2).

[51] **Geng, X. and Tam, H.W.** (1999). Darboux transformation and soliton solutions for generalized nonlinear Schrödinger equations, *Journal of the Physical Society of Japan*, *68*(5), 1508–1512.

[52] **Wang, P.**, **Tian, B.**, **Sun, K. and Qi, F.H.** (2015). Bright and dark soliton solutions and Bäcklund transformation for the Eckhaus–Kundu equation with the cubic–quintic nonlinearity, *Applied Mathematics and Computation*, *251*, 233–242.

[53] **Bayındır, C.** (2019). Self-localized solutions of the Kundu-Eckhaus equation in nonlinear waveguides, *Results in Physics*, *14*, 102362.

[54] **Bender, C.M.** (2015). PT-symmetric quantum theory, *Journal of Physics: Conference Series*, *631*, 012002.

[55] **Shabat, A. and Zakharov, V.** (1972). Exact theory of two-dimensional self-focusing and one-dimensional self-modulation of waves in nonlinear media, *Soviet physics JETP*, *34*(1), 62.

[56] **Yin, L.**, **Lin, Q. and Agrawal, G.P.** (2007). Soliton fission and supercontinuum generation in silicon waveguides, *Opt. Lett.*, *32*(4), 391–393.

[57] **Yang, J. and Lakoba, T.I.** (2007). Universally-Convergent Squared-Operator Iteration Methods for Solitary Waves in General Nonlinear Wave Equations, *Studies in Applied Mathematics*, *118*(2).

[58] **García-Ripoll, J.J. and Pérez-García, V.M.** (2001). Optimizing Schrödinger Functionals Using Sobolev Gradients: Applications to Quantum Mechanics and Nonlinear Optics, *SIAM Journal on Scientific Computing*, *23*(4), 1316–1334.

[59] **Yang, J. and Lakoba, T.I.** (2008). Accelerated Imaginary-time Evolution Methods for the Computation of Solitary Waves, *Studies in Applied Mathematics*, *120*(3), 265–292.

[60] **Yang, J.** (2009). Newton-conjugate-gradient methods for solitary wave computations, *JOURNAL OF COMPUTATIONAL PHYSICS*, *228*(18), 7007–7024.

[61] **Orszag, S.A.** (1971). Accurate solution of the Orr–Sommerfeld stability equation, *Journal of Fluid Mechanics*, *50*(4), 689–703.

[62] **Fornberg, B. and Whitham, G.B.** (1978). A numerical and theoretical study of certain nonlinear wave phenomena, *Philosophical Transactions of the Royal Society of London. Series A, Mathematical and Physical Sciences*, *289*(1361), 373–404.

[63] **Trefethen, L.N.** (2000). *Spectral Methods in MATLAB*, Society for Industrial and Applied Mathematics.

[64] **Boyd, J.P.** (2001). *Chebyshev and Fourier spectral methods*, Courier Corporation.

[65] **Milewski, P.A. and Tabak, E.G.** (1999). A PseudoSpectral Procedure for the Solution of Nonlinear Wave Equations with Examples from Free-Surface Flows, *SIAM Journal on Scientific Computing*, *21*(3), 1102–1114.

[66] **Strang, G.** (1968). On the Construction and Comparison of Difference Schemes, *SIAM Journal on Numerical Analysis*, *5*(3), 506–517.

[67] **Yanenko, N.N.** (1971). *The Method of Fractional Steps*, Springer Berlin Heidelberg.

[68] **Yoshida, H.** (1990). Construction of higher order symplectic integrators, *Physics Letters A*, *150*(5-7), 262–268.

[69] **Hall, B.** (2015). *Lie Groups, Lie Algebras, and Representations: An Elementary Introduction*, Graduate Texts in Mathematics, Springer International Publishing.

[70] **Kassam, A.K. and Trefethen, L.N.** (2005). Fourth-Order Time-Stepping for Stiff PDEs, *SIAM Journal on Scientific Computing*, *26*(4), 1214–1233.

[71] **Javanainen, J. and Ruostekoski, J.** (2006). Symbolic calculation in development of algorithms: split-step methods for the Gross–Pitaevskii equation, *Journal of Physics A: Mathematical and General*, *39*(12), L179–L184.

[72] **Lord, N.** (1999). Matrix computations, 3rd edition, by G. H. Golub and C. F. Van Loan. ISBN 0 8018 5414 8, 0 8018 5413 X. (Johns Hopkins University Press)., *The Mathematical Gazette*, *83*(498), 556–557.

CURRICULUM VITAE

Name Surname **:** Eril Güray ÇELİK

EDUCATION

- **B.Sc.** **:** 2018, Yildiz Technical University, Faculty of Chemical and Metallurgical Engineering, Department of Mathematical Engineering
- **M.Sc.** **:** 2022, Istanbul Technical University, Graduate School, Department of Mathematical Engineering

PROFESSIONAL EXPERIENCE:

- 2021-cont. Research Assistant at the Department of Computer Engineering at Dogus University.

PUBLICATIONS, PRESENTATIONS AND PATENTS ON THE THESIS:

- **Çelik, E.G., Antar, N.** 2021. Raman Etkisi ve Öz-Dikleşme Etkisi Altındaki Doğrusal Olmayan Schrödinger Denkleminin Soliton Çözümleri ve Kararlılık Analizi. *22. Ulusal Mekanik Kongresi*, 6–10 Eylül 2021, Adana, Türkiye.